IJCRT.ORG ISSN : 2320-2882

INTERNATIONAL JOURNAL OF CREATIVE RESEARCH THOUGHTS (IJCRT)

An International Open Access, Peer-reviewed, Refereed Journal

EVALUATION OF PAVEMENT USING GEOCELLS

[1]Cadirvelou K J, [2]Chitranjan Kumar

[1]Post Graduate Student, School of Engineering and Technology, Sri Venkateshwara University, Gajraula, Uttar Pradesh

[2]Assistant Professor, School of Engineering and Technology, Sri Venkateshwara University, Gajraula, Uttar Pradesh

Abstract : Highway Pavement structures frequently fail to reach their intended design life due to factors such as poor construction material quality, inadequate compaction, suboptimal subgrade preparation, and overloading. Addressing this challenge, two primary methods are considered in pavement design to enhance longevity: increasing the thickness of pavement layers or augmenting the rigidity of these layers to diminish stress transmission to lower layers. The latter method, increasing layer strength and rigidity, has been identified as a more effective strategy for extending pavement life. This paper focuses on the enhancement of the sub-base layer's strength and stiffness in a flexible pavement system through the application of geocell confinement. This paper endeavours to investigate the multifaceted aspects of pavement engineering with a primary focus on the incorporation of geocells as a potential solution. The research contextualizes the performance of highway pavements, which largely depends on the strength and stiffness of their layers. With the construction phase often constrained by the availability and cost of aggregate materials, and considering the increasing scarcity of natural resources leading to project delays and cost escalations, the study underscores the necessity of exploring alternative materials and methods. By utilizing geocells, the research proposes a sustainable approach to pavement design, aiming to achieve enhanced pavement quality with reduced reliance on natural materials, thereby addressing both economic and environmental concerns in pavement construction and maintenance.

Keywords : geocells, flexible pavement, economic and environmental concern in pavement construction and maintenance

I INTRODUCTION

1.1 Overview

Highway infrastructure is a critical component of India's development, with the demand for durable and cost-effective road networks continually rising. Traditional pavement designs, while effective, often face challenges in terms of longevity, environmental impact, and adaptability to diverse Indian climatic and geological conditions. The advent of geocell technology offers a promising alternative, potentially enhancing pavement performance while addressing these challenges. This project work seeks to provide an in-depth exploration of geocells in the context of highway engineering.

The study begins by assessing the structural benefits of geocells, hypothesizing that they can enhance the load-bearing capacity of pavements and potentially reduce the need for thicker conventional layers. Longevity and durability analysis forms a core part of the research, focusing on how geocells withstand India's unique traffic loads and environmental conditions. Alongside this, a cost-benefit analysis compares the initial and long-term expenses of geocell-incorporated pavements with traditional designs.

Environmental considerations are paramount; thus, the research investigates the ecological advantages of geocells, such as minimizing the use of non-renewable materials and incorporating recycled elements. The

performance of geocells under extreme weather conditions prevalent in India, including monsoons and temperature fluctuations, is also scrutinized.

Local material utilization is explored, assessing the compatibility of geocells with indigenous materials to reduce costs and environmental footprints. Furthermore, the impact of geocells on the construction process is examined, hypothesizing potential benefits in construction speed and reduced disruption. Ensuring that geocell-based pavement designs adhere to Indian Standard Codes and Indian Road Congress codes of practice is another critical objective.

The scalability and feasibility of geocells in varying Indian regions, each with distinct soil types and traffic conditions, are evaluated to understand their broad applicability. Additionally, the dissertation aims to adapt and refine existing pavement design methods to optimally include geocells, tailored to Indian conditions.

To support long-term adoption, a framework for ongoing monitoring and performance assessment is proposed, aiming to build a comprehensive database of performance metrics. Lastly, the study culminates in formulating policy recommendations and implementation strategies to integrate geocells into standard pavement design practices, paving the way for the upgrade of existing infrastructure.

This research, therefore, aims to provide a holistic understanding of the potential benefits and challenges of incorporating geocells in highway engineering in India, offering insights that could be instrumental in shaping future infrastructure development.

1.2 RESEARCH OBJECTIVES

Potential research objectives are as follows:

1.2.1 Assessing the Structural Benefits:

Evaluate how geocells contribute to the load-bearing capacity of pavement structures, potentially reducing the thickness of traditional pavement layers required to achieve the same performance.

1.2.2 Longevity and Durability Analysis:

Determine the impact of geocells on the lifespan of pavements under the specific traffic loads and environmental conditions prevalent in India.

1.2.3 Local Material Utilization:

Assess the effectiveness of geocells when used with locally available materials, which can significantly reduce the cost and carbon footprint associated with transportation of materials.

1.2.4 Environmental Impact:

Investigate the environmental benefits of using geocells, such as reduced need for non-renewable materials and the potential for incorporating recycled materials within the geocell structure.

1.3 SIGNIFICANCE OF STUDY

The study on the evaluation of pavement design using geocells is highly significant, especially in the context of highway infrastructure works like those in India. This study intersects various aspects of highway engineering and sustainable transportation planning. Here's a detailed look at its significance:

1.3.1 Improved Pavement Performance:

Geocells, due to their three-dimensional honeycomb-like structure, provide excellent confinement for the infill materials. This can significantly improve the load distribution on the pavement, leading to enhanced performance in terms of durability and resilience.

1.3.2 Cost-Effectiveness:

By enhancing the load-bearing capacity of the subgrade, geocells can reduce the thickness of traditional pavement materials required, potentially leading to cost savings in materials and construction.

1.3.3 Sustainability:

The use of geocells aligns with sustainable transportation planning goals. It can lead to the use of locally available and less environmentally damaging materials, reducing the carbon footprint of highway construction and maintenance.

1.3.4 Adaptability to Indian Conditions:

Considering the diverse terrain and climatic conditions in India, the adaptability of geocells to different types of soil and environmental conditions makes them a versatile solution for pavement design.

1.3.5 Longevity and Maintenance:

The increased stability and strength provided by geocells can lead to longer-lasting pavements with reduced maintenance needs, which is crucial for effective project management in highway infrastructure.

1.3.6 Application in Traffic Management Systems:

Improved pavement quality can lead to better traffic flow and reduced congestion, indirectly contributing to more effective traffic management systems.

1.3.7 Research and Innovation in Highway Engineering:

This research contributes to the field of highway engineering, particularly in understanding and optimizing the use of modern materials and technologies in pavement design.

1.3.8 Alignment with Intelligent Transportation Systems (ITS):

Better pavement design can support the infrastructure needs of ITS, providing a more reliable base for the implementation of advanced technologies in transportation systems.

1.4 METHODOLOGY

The methodology for the project to be structured as follows:

1.4.1 Literature Review

Objective: Gathering existing knowledge and previous research findings on pavement design, particularly focusing on the use of geocells.

Activities: Reviewing academic journals, industry reports, and case studies related to pavement engineering, geocell applications, and material science.

1.4.2 Hypothesis Formulation

Objective: Developing a hypothesis based on the literature review about how geocells might improve the strength and longevity of pavement designs.

Hypothesis Example: "Incorporating geocells in pavement design will significantly increase the strength and stiffness of the sub-base layer, leading to longer pavement life."

1.4.3 Design of Experiment

Objective: To plan and design experiments that will test the hypothesis.

Components:

- Selection of materials including types of geocells.
- Identification of control variables (e.g., soil type, traffic load).
- Design of test sections (with and without geocells).

1.4.4 Laboratory Plate Load Tests

Objective: To conduct controlled experiments to understand the mechanics of geocell reinforcement.

Procedure:

- Simulate pavement layers in laboratory conditions.
- Apply controlled loads and measure responses.
- Compare results with field tests for consistency.

1.4.5 Data Collection and Analysis

Objective: To collect and analyse data from both field and laboratory tests.

Methods:

- Use sensors and measuring instruments for accurate data collection.
- Apply statistical and engineering analysis methods to interpret the data.
- Evaluate the increase in modulus of elasticity and other relevant parameters.

1.4.6 Application to Pavement Design

Objective: To translate findings into practical pavement design applications.

Activities:

- Develop guidelines for incorporating geocells in pavement design.
- Conduct cost-benefit analysis comparing traditional and geocell-reinforced designs.
- Address scalability and environmental impact.

1.4.7 Conclusions and Recommendations

Objective: To draw conclusions from the research and make recommendations for future pavement designs.

Elements:

- Summarize key findings and their implications for pavement longevity and strength.
- Suggest areas for further research.
- Propose recommendations for the implementation of geocells in real-world pavement designs.

II OVERVIEW OF PAVEMENT DESIGN

Roadway pavements play a very important role in the nation's economic activity. Approximately, 19% of average household expenditures is directly related to transportation. The predominant mode of personal transportation is by private motor vehicle, that is, 91.2% of the total vehicle-kilometres [6]. Furthermore, an average 89% of commercial freight transportation is carried by the highway system. The vehicle-miles travelled (VMT) is a very good indicator of the health of the economy, as suggested by its strong correlation to the gross domestic product (GDP), that is, the annual sum of goods and services transacted nation-wide. These simple facts demonstrate the importance of the roadway infrastructure in the nation's economic well-being [5].

Highway pavement refers to the durable surface material laid on the topmost layer of a road or highway, designed to withstand traffic loads and provide a smooth, safe, and efficient driving surface. It's a crucial component of transportation infrastructure, ensuring the longevity and functionality of our roadways.

A highway pavement is a structure consisting of superimposed layers of processed materials above the natural soil sub-grade, whose primary function is to distribute the applied vehicle loads to the sub-grade. The pavement structure should be able to provide a surface of acceptable riding quality, adequate skid resistance, favourable light reflecting characteristics, and low noise pollution. The ultimate aim is to ensure that the transmitted stresses due to wheel load are sufficiently reduced, so that they will not exceed bearing capacity of the sub-grade. Two types of pavements are generally recognized as serving this purpose, namely flexible pavements and rigid pavements. Improper design of pavements leads to early failure of pavements affecting the riding quality.

Pavement deterioration is caused by the interacting damaging effects of traffic and the environment. Traffic loads, primarily those from heavy trucks, cause stresses/strains in pavement structures, whose effects accumulate overtime, resulting in pavement deterioration, such as plastic deformation in asphalt concretes or fatigue cracking in Portland concretes. Hence, truck traffic load data is an essential input to the pavement analysis and design process. Truck traffic loads and their impact on pavements are quantified in terms of:

- Number of truck axles
- Configuration of these axles
- Their load magnitude

A highway pavement is a structure consisting of superimposed layers of processed materials above the natural soil sub-grade, whose primary function is to distribute the applied vehicle loads to the sub-grade. The pavement structure should be able to provide a surface of acceptable riding quality, adequate skid resistance, favourable light reflecting characteristics, and low noise pollution. The ultimate aim is to ensure that the transmitted stresses due to wheel load are sufficiently reduced, so that they will not exceed bearing capacity of the sub-grade. Two types of pavements are generally recognized as serving this purpose, namely flexible pavements and rigid pavements. Improper design of pavements leads to early failure of pavements affecting the riding quality.

2.2 Requirements of a Pavement

An ideal pavement should meet the following requirements:

- Sufficient thickness to distribute the wheel load stresses to a safe value on the sub-grade soil,
- Structurally strong to withstand all types of stresses imposed upon it,
- Adequate coefficient of friction to prevent skidding of vehicles,
- Smooth surface to provide comfort to road users even at high speed,
- Produce least noise from moving vehicles,
- Dust proof surface so that traffic safety is not impaired by reducing visibility,
- Impervious surface, so that sub-grade soil is well protected, and
- Long design life with low maintenance cost.
- Pavement design in highways is a critical aspect of road construction, ensuring the durability and safety of the road for its intended lifespan. The primary function of pavement is to distribute the loads from vehicles to the underlying soil, preventing excessive deformation and distress.

2.3 Pavement Structure

Pavement structure is a part of road structure, which consists of the following elements: subgrade, subbase course, base course, and asphalt layer, all of which directly bear the effects of heavy loads and environmental conditions. The basic requirements for pavement are durability, smoothness, and safety (i.e., skid resistance). Pavement should also be constructed in a way that is as friendly to environment as possible. Durability means longer service life; that is, the pavement structure must have enough strength and resistance to deformation.

The properties of the base/subbase and subgrade layers play a vital role in the structural integrity and performance of pavements. In flexible pavements, the base and subbase layers are structural components that need to provide sufficient strength, while reducing stresses to levels that can be sustained by the subgrade. In rigid pavements, the base layer is used for levelling and structural strengthening of weak subgrades. Furthermore, properly constructed base/subbase layers can provide internal drainage, while preventing water ingress into the subgrade. The properties of the subgrade and base layers can be improved through compaction or chemical stabilization under controlled moisture conditions.

2.4 Philosophy of Pavement Design

The philosophy of pavement design involves designing pavements for satisfactory functional and structural performance of the pavement during its intended service life period. Roughness caused by variation in surface profile, cracking of layers bound by bituminous or cementitious materials, rutting (permanent or plastic deformation) of unbound/unmodified or partially modified subgrade, granular layers and bituminous layers are the primary indicators of the functional and structural performance of pavements. Performance of the pavement is explained by performance models which are either (a) purely empirical (only based on past experience) or (b) mechanistic-empirical, in which the distresses/performance are explained in terms of mechanistic parameters such as stresses, strains and deflections calculated using a specific theory and as per a specified procedure. Most of the current pavement design methods follow the mechanistic empirical approach for the design of bituminous pavements. In these methods, for each of the selected structural distresses, a critical mechanistic parameter is identified and controlled to an acceptable (limiting) value in the design process. The limiting values of these critical mechanistic parameters are obtained from the performance models.

Flexible pavements are modelled as layered elastic systems with infinite lateral dimensions. These layers rest on the subgrade, which is often modelled as an elastic layer of infinite depth. Elasticity implies that all the pavement layers and the subgrade can be described by their elastic Young's modulus E and their Poisson's

ratio μ. Furthermore, the layers are assumed to be homogeneous and isotropic. Tire loads are modelled as either point loads or circular loads of uniform pressure using mathematical Equations. Under these conditions, the stress state is axisymmetric; that is, it exhibits rotational symmetry around the center axis of the load and, as a result, it is easier to describe using a radial coordinate system. Pavement responses, (i.e., stress, strains, and deflections) are calculated using relationships from the theory of elasticity. The responses from multiple loads are calculated by superimposing the stresses from the individual tires, according to D'Alembert's superposition principle. Analysing these responses is essential for the mechanistic design of asphalt concrete pavements.

Flexible pavements will transmit wheel load stresses to the lower layers by grain-to-grain transfer through the points of contact in the granular structure. The wheel load acting on the pavement will be distributed to a wider area, and the stress decreases with the depth. Taking advantage of this stress distribution characteristic, flexible pavements normally have many layers. Hence, the design of flexible pavement uses the concept of layered system. Based on this, flexible pavement may be constructed in several layers and the top layer has to be of best quality to sustain maximum compressive stress, in addition to wear and tear. The lower layers will experience lesser magnitude of stress and low-quality material can be used. Flexible pavements are constructed using bituminous materials. These can be either in the form of surface treatments (such as bituminous surface treatments generally found on low volume roads) or asphalt concrete surface courses (generally used on high volume roads such as national highways). Flexible pavement layers reflect the deformation of the lower layers on to the surface layer (e.g., if there is any undulation in sub-grade then it will be transferred to the surface layer). In the case of flexible pavement, the design is based on overall performance of flexible pavement, and the stresses produced should be kept well below the allowable stresses of each pavement layer.

The philosophy of rigid pavement design involves understanding the behaviour of rigid pavements under various loading conditions and environmental factors. As the name implies, rigid pavements are rigid i.e., they do not flex much under loading like flexible pavements. They are constructed using cement concrete. In this case, the load carrying capacity is mainly due to the rigidity ad high modulus of elasticity of the slab (slab action). H. M. Westergaard is considered the pioneer in providing the rational treatment of the rigid pavement analysis. Rigid pavements are typically constructed using concrete slabs, which are designed to transfer loads to the subgrade through flexural action. The main objective of rigid pavement design is to ensure that the pavement can withstand the anticipated traffic loads and environmental conditions without excessive cracking, faulting, or other forms of distress.

The performance of highway pavements is governed by the strength and stiffness of the pavement layers. The cost and duration of construction are dependent on the availability of aggregate for construction. Scarcity of natural resources often delays the projects or escalates the costs due to large lead distances from the borrow areas. Hence it is essential to look at alternatives to achieve improved quality of pavements using new materials and reduced natural material usage.

2.5 Need of Geocell in Pavement Design

Nowadays, many of the flexible pavement structures fail to meet their design life due to unequal settlement and disintegration of layers. Many roads have a prime problem like lack of soil stability, disintegration, settlement and so on. Disintegration is the process of progressive breaking up of the pavement into small, loose pieces. Due to continuous vehicle movement, and poor drainage, peeling off of bitumen surface takes place, causing migration of the gravel below it to other areas. Passing over the time it can gradually reduce the level of pavement and create ruts, dips, and holes in the driveway. Potholes or craters are the major problem. In this project, we focus on design of flexible pavement to improve the strength and stiffness of subbase layer of flexible pavement by using geocell confinement. Geocell is a 3D honey combed polymer matrices formed by interconnected cells. Three types of infill materials used here are quarry waste, clay and aggregate. The test result shows that geocell confinement can reduce the permanent deformation of settlement and increase the elastic deformation of granular bases. Sustainable paved road can help to face these challenges by improving the long-term road strength and rigidity. Geocell, a cellular confinement. The cells are filled with the selected infill material, the proper bond between the cell and infill material can improve pavement strength by lateral vertical confinement. Hence, frictional resistance between the infill and cell wall increases and prevent restrained soil from moving upward outside the loading area. Geocells can be installed easily, and requirement of skilled labour is not there. Easily transportable as flat strips welded width wise at regular intervals. They can be installed in any weather condition; geocells substantially reduce construction

time and maintenance cost by improving the longevity of the road / pavement. Considering all the above, HDPE geocells help to reduce carbon footprint, since carbon black is an essential ingredient of the HDPE.

Pavements, which are functionalised for transmitting the vehicle wheel load to deeper competent soil strata in order to provide safety, are categorised into two types, namely flexible pavement and rigid pavement. Flexible pavement is a load-carrying structure, which consists of layers of various granular materials above the subgrade material. The primary aim of flexible pavements is to create a safe driving surface without any inconvenience for passengers and vehicles due to the extreme deformation of the pavement structures. The durability of flexible pavements depends on different factors, such as the pavement layer thicknesses, strength of the subgrade, stiffness of the various pavement layers, and environmental conditions. In recent years, many roads have been designed on weak subgrade (California bearing ratio < 5%) as the amount of road traffic has increased. Such tasks are difficult for engineers as weak subgrade soil has a low shear strength, causing excessive consolidation, bearing capacity failure, and insufficient load transfers from the base layer when subjected to heavy, repeated traffic loads. Thus, a weak subgrade was a major concern for pavement design engineers because of its potential contribution to large permanent deformation in flexible pavements. Such a problem has contributed to research efforts to enhance the condition of the pavement structure and to establish sustainable.

The nature of soil presents around the world is of many varieties ranging from stiff to weak and dense to loose. Since the availability of good construction site is limited, in spite of how weak the soil is, there is need to improve such sites, when it is not possible to avoid such sites. Use of geocell has been gaining advantages over the other improvement methods. . A few examinations considered, have appeared in the past that the geocells support is viable when a granular infill is utilized over frail subgrades. Studies were performed on the flexible pavement with and without geocell strengthened basal layer under static and repeated loading. There is a need to comprehend the conduct of geocell confined granular total bases over frail subgrades under repetitive traffic loading. Rutting is a typical phenomenon experienced in flexible pavement upheld by frail subgrades.

Reinforcing the weak subgrades with geocells are one of the best methods to counter the base surface rutting. Research studies have satisfied that inclusion of geocells can reduce rut depth to a greater extent as well as it may be utilized for soil control to give extra quality and firmness to the base coarse.

Ground improvement using the soil reinforcement technique has grown substantially in the last three decades. The technique has grown from use of metal grids to use of geosynthetic products such as geogrids and geocells to reinforce soft soil. Nowadays, geocells are being widely used in geotechnical engineering to strengthen soft soil. General applications of geocell include pavements, foundations, and embankments. By virtue of its three-dimensional (3D) box-like structure, geocell provides additional confinement to the soil. Geocells offer faster, cheaper, sustainable, and environmentally friendly solutions to many complex geotechnical problems. Many researchers have highlighted the beneficial effects of the geocells with the help of 1g model tests *(Sitharam et al. 2005; Dash et al. 2007; Moghaddas Tafreshi and Dawson 2010; Dash and Bora 2013; Tanyu et al. 2013; Hegde and Sitharam 2014a; Hegde et al. 2014).* Some researchers in the past also studied the efficacy of geocells using the full-scale field tests and the case studies *(Cowland and Wong 1993; Han et al. 2011; Kief et al. 2011; Yang et al. 2012; Moghaddas Tafreshi et al. 2013, 2014; Sitharam and Hegde 2013)*. However, very few researchers have attempted the numerical modelling of the geocells due to difficulty in modelling its complex honeycomb structure. Because geocell applications are growing at a rapid rate nowadays; it is high time to demonstrate the realistic approach of modelling the geocells. The design computations often require quick calculations to understand the effect of the various key parameters in the design.

In such situations, one cannot always depend on the experimental and field studies. Numerical modelling technique not only helps to carry out quick calculations, but also provides the scientific representation of the results. In the recent past, the geocells have been modelled using the equivalent composite approach and in which the geocell–soil composite is treated as the soil layer with improved strength and stiffness values *(Bathurst and Knight 1998; Madhavi Latha and Rajagopal 2007; Madhavi Latha and Somwanshi 2009; Hegde and Sitharam 2013; Mehdipour et al. 2013).* Though this approach is very simple, it is unrealistic to model geocells as the soil layer. Because geocells have a 3D structure, it is always appropriate to model them in a 3D framework. Han et al. (2008) carried out the numerical simulation of a single cell geocell subjected to uniaxial compression in FLAC3D. In their study, the cell was modelled as the square box due to the difficulty in modelling the actual shape. For the same reason, Hegde and Sitharam (2014b) adopted the circular

shaped pocket geometry while modelling the problem of the single cell geocell subjected to uniaxial compression. In their study, the researchers observed the deviation in the experimental and numerical pressure–settlement response at the higher settlement. The researchers had attributed this anomaly to the circular shaped geometry used in the modelling process and emphasized the importance of modelling the actual shape of the geocells. *[Saride et al. (2009)]* adopted the square shaped geometry of the cell pocket while modelling the multiple cell geocell in FLAC3D. A similar approach was also used by Leshchinsky and Ling (2013) while modelling a geocell reinforced ballast system. However, the actual shape (i.e., 3D honeycombs shape) of the single cell geocell was modelled by *Yang et al. (2010)* in their study.

Contrary to the previous studies, an attempt has been made to model the real shape of the multiple cell geocells by considering the actual curvature of its pocket. The foundation soil, infill soil, and the geocell materials were assigned with three different material models to simulate the real case scenario. To validate the numerical modelling, the laboratory plate load tests were conducted on soft clay bed reinforced with geocells. The validated numerical model was further used to study the influence of the various geocell properties on the performance of the reinforced clay beds.

III BRIEF ABOUT GEOCELLS

Since the 1970s, geocells are being widely used in various applications of geotechnical engineering. The idea of a cellular confinement system was originally developed by US army corps of engineers for the ease of transport of military vehicles over weak subgrades. The first cellular confinement systems were made of paper, which were later replaced by aluminium and wooden cells. An early version of geocells, which were called sand grids made of plastic or aluminium used by US Waterways Experimentation Station at Vicksburg, MS, USA in 1979, as illustrated by Webster, is shown in Figure 3.1.

The modern form of geocells came into existence since 1980s. Unlike planar textiles and grids, geocells, which are three-dimensional networks of cells filled with a choice of soil, provide added benefits such as all-round confinement through hoop stresses developed in the cells and a beam effect resulting from their stiff-mat configuration. Geocells, by virtue of their shape and depth, provide greater load-bearing capacity and

Figure 3.1 Early version of Geocells used by US Waterways, Experimentation Station at Vicksburg, MS, USA

reduce lateral deformations in soils confined by them under static and cyclic loading scenarios.

The inclusion of geocells in various structures has additional benefits such as stability improvement, climate resilience, higher resistance to cyclic loads, erosion control, basal support, and savings in time and cost. Because of these merits, geocells are extensively used in pavements, slopes, foundations, embankments, and reinforced earth (RE) walls.

Recently, geocells have also found application in heavy-duty highways and high-speed trains.

The mechanism of geocell reinforcement has been investigated by many researchers through experimental, numerical, and analytical studies. In a network of geocells, each cell is surrounded by several neighbouring cells, and all the cells are filled with soil. With the application of external load, the soil inside the geocell pushes the cell wall, resulting in the development of an additional confining stress along the wall. The additional confinement is translated into apparent cohesion, thereby increasing the shear strength of the soil, and preventing its lateral spread. Furthermore, the extension of cell walls is opposed by the lateral stresses from the neighbouring cells, causing the interconnected network of geocells to act as a cushion or stiffened mattress with higher strength and stiffness. This beam action redistributes the externally applied loads over a wider area and, thus, reduces the magnitude of stresses acting on the underlying soil. This stiffened soil–

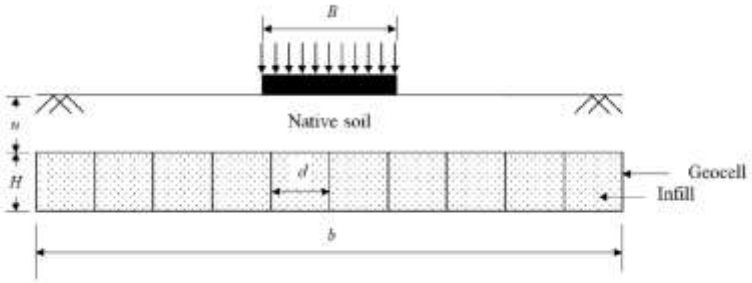

geocell composite also hinders the propagation of the failure surface into the underlying soil. Furthermore, at large displacements, the geocell layer acts as a tensioned membrane, providing sufficient upward resistance to the applied loads and, thus, reducing the stresses on the underlying soil. A schematic representation of a geocell-reinforced soil bed is shown in Figure 3.2.

Figure 3.2. Schematic representation of geocell reinforced foundation bed

In this figure, B represents the width of the foundation, u represents the depth of the geocell layer from the ground surface, and H, d, and b represent the height, pocket size, and width of the geocell layer, respectively.

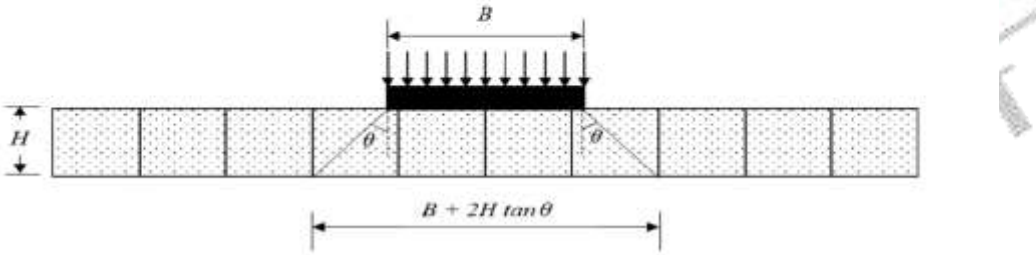

Various mechanisms responsible for the reinforcing action of geocells are presented in Figure 3. In this figure, ‘θ’ represents the angle of load dispersion.

Figure 3.3 Stress dispersion effect (sectional elevation)

Figure 3.4 shows a photograph of the latest form of commercially available honeycomb shaped geocells available at the Indian Institute of Science, Bangalore. Figure 3.4a shows the collapsed form of geocells, which helps in stacking large volumes of geocells in a compact form. In Figure 3.4b, an expanded form of a geocell layer is shown, and the cell wall, junctions, and perforations are marked. Geocells took almost five decades to evolve geometrically to their current versatile configuration. Historically, geocell layers were fabricated onsite using planar geosynthetics such as geotextiles and geogrids by strategically connecting the cells and filling them with granular soils. Initially, resins and additives were used to connect the cells, which were chronologically replaced by bodkin joints, photo lamination, and ultrasonic welding in the most recent form of commercial geocells. Similarly, the geometric shape of the geocells has also undergone several

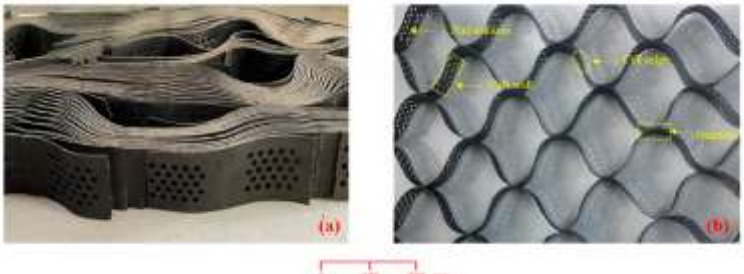

transformations from square, circular, rectangular, diamond, and hexagonal to honeycomb. Furthermore, the cell material also evolved from paper, aluminium, and wood to polymer. Currently, solid or perforated high-density polyethylene (HDPE) and novel polymeric alloy (NPA) are the commonly used polymers to manufacture geocells. However, the latter is more popular due to its greater flexibility, thermo-plasticity, and surface texture.

Figure 3.4. Commercially available Geocells (a) Collapsed form (b) Expanded form

The present-day configuration of honeycomb geocells enables them to enclose maximum infill with a minimum perimeter of cells. While manufacturing geocells, surface texture is imparted to the geocells, as shown in Figure 4, to enable them to mobilize greater interfacial shear strength when they are in contact with soils. The postmortem analysis of geocells from various model tests showed that the junctions of the geocells remained intact even when local straining and buckling were observed in geocell walls. Furthermore, the perforations present on the geocell walls facilitate easy drainage to dissipate pore pressures that develop inside the cells. These perforations also provide adequate interlocking between infill soils of adjacent geocells so that the geocell reinforced soil behaves like a stiffened composite mass. The perforations on cell walls also facilitate root growth within the cells, which is beneficial when vegetation is grown on geocell walls and slopes. The total pore area of the perforations is typically 6–22% of the unit area of the geocell wall. Table 1 presents the typical range of geometric and mechanical properties of commercial geocells reported by earlier studies and geocell manufacturing companies.

Table 3.1 Typical properties of Commercial Geocells

Property	Value
Density	0.932 to 0.95 g/cm^3
Strip Width	50 – 300mm
Strip Thickness	1.53mm (±10%)
Percentage of perforations to cell area	6 – 22%
Ultimate Tensile Strength	16 – 25 kN/m
Junction Peel strength	7 – 10 kN/m
Elongation at maximum load	20% (±15%)
Dynamic modulus at service temperature (-60ºC to 60ºC)	650 – 800 MPa
Resistance to ultraviolet degradation	250 – 400 min
Cumulative permanent deformation (creep resistance)	2.7 – 3.5%

3.2 Geocell Configuration

The reinforcement efficiency of geocells is mainly governed by the geocell configuration, geocell material properties, and soil properties. This section presents a detailed discussion on the evolution of geocells with variations in the parameters grouped under these three categories. Various studies that dealt with the variation in geocell geometry and configuration are reviewed, and the individual and combined effects of these parameters are discussed in light of the published papers. The geocell configuration mainly pertains to the shape, size, quantity, and location of geocells. The various factors that define the configuration are the height (H), overall width (b), pocket shape, and pocket opening size (d), which is the diameter of the equivalent circle, the pattern of arrangement in the case of geocells made of geogrids, embedment depth (u), and the

number of geocell layers, as depicted in Figure 3.5. Since geocells improve strength through friction and interlocking, their height, width, and pocket size play a pivotal role in their reinforcing action. The number of

geocell layers (N) becomes an important parameter only at higher levels of external loads applied on weak soils.

Figure 3.5. Schematic representation of Geocell geometry

IV LITERATURE REVIEW

4.1 Overview

Pavement construction is the single largest market of natural aggregates. Aggregates constitute about 100% of base and subbase courses, 87% of Portland cement concrete pavements and 95% of bituminous pavements. The amount of aggregate required for a km of a surface course of bituminous mix can exceed 15,000 tons. The massive demand of aggregates resulting from rapid urbanization in India has already started taking its toll - there are many areas where aggregates need to be transported from hundreds of km away for construction of new roads, for maintaining and rehabilitating existing roads. Furthermore, with concerns about pollution, opening up of new quarries are becoming increasingly difficult. Transportation of aggregates over long distances adds to fuel cost and contributes to increase in emissions. Hence the depletion of stock of natural aggregates has a huge impact on costs, as well as the environment. How big is the impact? If, instead of using natural aggregates, one started recycling of existing roads for maintenance and rehabilitation, what will be the reduction in the impact? How much recycling needs to be done and how soon? This paper attempts to answer these questions with the help of system dynamics modelling. The conclusions are alarming and demand an immediate and serious consideration of policies to allow and enable recycling of pavements in India.

Pavements, which are functionalised for transmitting the vehicle wheel load to deeper competent soil strata in order to provide safety, are categorised into two types, namely flexible pavement and rigid pavement. Flexible pavement is a load-carrying structure, which consists of layers of various granular materials above the subgrade material. The primary aim of flexible pavements is to create a safe driving surface without any inconvenience for passengers and vehicles due to the extreme deformation of the pavement structures. The durability of flexible pavements depends on different factors, such as the pavement layer thicknesses, strength of the subgrade, stiffness of the various pavement layers, and environmental conditions. In recent years, many roads have been designed on weak subgrade (California bearing ratio < 5%) as the amount of road traffic has increased. Such tasks are difficult for engineers as weak subgrade soil has a low shear strength, causing excessive consolidation, bearing capacity failure, and insufficient load transfers from the base layer when subjected to heavy, repeated traffic loads. Thus, a weak subgrade was a major concern for pavement design engineers because of its potential contribution to large permanent deformation in flexible pavements. Such a problem has contributed to research efforts to enhance the condition of the pavement structure and to establish sustainable strategies for stabilising pavement. One way to address this concern is to incorporate enough reinforcement to boost the overall strength and rigidity of the pavement structure while also minimising related expenditures. Geosynthetic material has significantly contributed to enhancing the efficiency of both unpaved and paved roads over the last 40 years and has been one of the verified base course reinforcement strategies.

Several geosynthetic materials have been developed to enhance soil quality and performance in a variety of pavement-related applications, including base and subbase stabilisation, strengthening, drainage, slope protection, and embankment protection. In recent years, geocells have been widely employed to build low-maintenance roadways in problematic ground conditions. Among various geosynthetic materials, geocell (as depicted in Fig. 4) is a three-dimensional geosynthetic product composed of high-density polyethylene, polyester, or other polymers.

The connected cells were filled with granular materials to create a stiff base for supporting the different loading conditions. The lateral confinement to the infill material within the cells was generated due to the interfacial friction between the geocell and infill material. Therefore, the geocell-soil layer reduces the vertical and lateral deformation of subgrade soil by distributing the load over a larger area of subgrade soil. Consequently, geocells in flexible pavements increase the load-bearing capability and service life of the pavement. The schematic diagram of geocell reinforced flexible pavement is shown in Fig. 4.1.

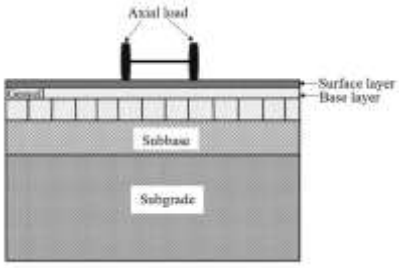

Figure 4.1. Schematic representation of geocell-reinforced pavement

Extensive research was conducted in the laboratory to investigate the effect of geocell in reinforced pavement. However, there have been relatively limited field trials and numerical studies aimed at providing insights into the behaviour of geocell-reinforced soil. The findings from these studies indicate that the application of geocells is advantageous for a variety of geotechnical engineering tasks *[Geocell as a Promising Reinforcement Technique for Road Pavement: A State of the Art Sayanti Banerjee1, Bappaditya Manna1,J. T. Shahu]*

The case selected was the reconstruction of a road that showed excessive rutting. The use of geocells was chosen as the solution on an experimental basis, and the results showed that the pavement laid on the confined base showed no signs of rutting. *Emersleben and Meyer (2008)* conducted large scale model tests and field tests which showed similar results which verified the fact that geocells reduce surface deflections and vertical pressure on the subgrade. The tests also studied the effect of aspect ratio and results showed that performance improved as the height to diameter ratio was increased. Geosynthetics firm Strata Geosystems (India) has been providing case histories for the use of its products. Their geocell product was used in the construction of State Highway Road for Kumbakonam – Mannargudy, Chennai-Kanniyakumari Industrial Corridor Project, Tamil Nadu. At the end of the study period, it was found that the use of geocells not only reduced the material required, but also improved the speed of construction. Along with the field tests, *Emersleben and Meyer (2008)* also conducted large scale model tests in test boxes measuring 2m x 2m x 2m. The tests showed that the surface deflection is lesser in a geocell confined section, and the results were verified by FWD measurements carried out in field studies. *Rajagopal et al. (2001)* proposed the following equation for the layer modulus of geocell-confined sand (E.g.) in terms of the secant modulus of the geocell material and the modulus parameter of the unreinforced sand *(Ku)*:

Here *"Pa"* is the atmospheric pressure, *"Ku"* is the modulus number for unreinforced soil *(Duncan and Chang, 1970)* and "M" is the secant modulus of geocell material in kN/m and σ3 is the confining pressure.

4.2 STUDIES ON GEOCELL REINFORCEMENT UNDER STATIC LOAD

The studies on a 3-dimensional reinforcing structure named geocell was introduced considering the additional function of confinement along with the various functions provided by planar geo-synthetics like geo-grids and geo-textiles. *Bush et al.* carried work on the design and construction of geocell foundation mattress supporting embankments over soft grounds. They concluded that the differential and total settlements were reduced due to load distribution through geocell mattress. The study also reported that the cost saving up to 30% can be achieved by constructing geocell reinforced embankment over soft soil as compared to conventional methods. Several researchers *(Barksdale; Cowland and Wong; Cancelli,; Collin, Dash et al.; Sitharam and Sireesh*, have done extensive study on the geocell reinforced beds under static loading conditions to understand the behaviour of geocell mattress and have successfully quantified the improvements mainly in terms of increased bearing capacity of footing. Saride et al. and Han et al. reported that the geocell reinforcement proved effective in increasing the bearing capacity of footings because of the lateral confinement of the cell in case of a geocell under static loadings. It was observed that the placement of geocell from the surface of loading is also an important factor in improving the performance of reinforced beds. Studies performed by Dash et al and Sitharam and Sireesh suggested that the placement depth of geocell

should be maintained about 1 to 5% of the width of the loading area in static load tests. Dash et al. performed model studies on circular footing supported on geocell reinforced sand placed on soft clay subgrades and concluded that the performance of the test beds can be improved drastically by employing geocells in a dense sand layer. They also observed about 80% reduction in footing settlements when an optimum size of geocell (width ratio, b/D = 5 and height ratio, h/D = 2.1) was used. A seven fold increase in the bearing capacity was achieved for the optimum size of geocell mattress employed. Similarly, Mandal and Gupta [20] analysed the performance of geocell, when placed in a sand layer underlying marine clay by performing laboratory tests and observed an improvement in the bearing capacity of the marine clay overlain by sand layer. From their study they concluded that the geocell with smaller opening size is found to be an appropriate reinforcement for paved roads with very less permissible settlements, whereas in the case of unpaved roads, large size geocells are observed to be effective. Table 4.1 summarizes the various studies performed by the researchers on the effectiveness of geocell mattress in improving the bearing capacity of the weak foundation beds.

Table 4.1 Summary of studies performed on geocell mattress under static loading condition

Study	Type of Facility	Geo-synthetics Used	Remarks
Bush et al.	Embankment	Geocell	Enhanced bearing capacity.
Cowland and Wong	Embankment on soft clay	Geocell	Enhanced bearing capacity
Mhaiskar and Mandal	Soft Clay Subgrade	Geocell	improvement in the ultimate load and reduction in settlement
Krishnaswamy et al.	Embankments constructed over soft clay bed	Geocell	Results depend on Stiffness of the geocell, pocket opening size, height of geocell, type of soil filled inside the geocell, and the pattern used to form the geocells.
Dash et al.	Laboratory tank	Geocell	Enhanced bearing capacity of strip footing on sandy ground
Saride et al.	Laboratory tank	Geocell	Substantial increase in the bearing capacity and reduce settlement of the clay and sand subgrades under circular loading
Hegde et al.	Laboratory tank	Geocell	The load carrying capacity of the geocell reinforced bed increased by 13 times for the aggregate in fill, 11 times for the sand infill and 10 times for the red soil infill.

4.3 Studies on Geocell Reinforcement under repeated loads

The studies on the geo-synthetic reinforcement were started about five decades ago. Different reinforcement forms are being used for a long time viz. geo-textiles, geo-grids, geonets, geo-composites and geocells. Extensive literature is available on these materials as reinforcement (geo-grids and geocells) under static loading for pavement applications however, a very few studies are available on cyclic loading. Understanding of these mechanisms originated from static plate load tests, but later research has been focused on these mechanisms under cyclic loading.

It was noticed that the ultimate bearing capacity increases with increasing number of reinforcement layers under dynamic loading. Depth of placement of initial reinforcement and spacing between consecutive layers were kept constant (u/D = h/D = 0.33) for all tests. Also, width of geo-synthetic reinforcement was maintained four times width of model footing. It was observed that increase in reinforcement layer (beyond N = 4) does not enhance the improvement in bearing capacity. Dynamic load tests were conducted based on the optimum configuration obtained from static load test. Dynamic load was applied using a 16 rectangular shaped waveform and frequency of 1 Hz. Tests were conducted in a rigid stee1 tank measuring 760 mm from all sides and a square shaped rigid footing of side 76.2 mm *(Halliday and potter)*.

4.4 STUDIES ON DESIGNING PAVEMENTS WITH GEO-SYNTHETICS

The design methods presently available for use of geo-grids in road base stabilization provide no or insufficient information about the required number of layers and the mechanical characteristics of geo-grids. Hence, a new design method has been developed which includes the design of geo-grids for road base stabilization, based on a four layer model: asphalt (binder and wearing course), base, subbase and subgrade. The base and/or subbase thickness has to be defined with one of the available methods such as AASHTO method, Giroud–Han method, Leng – Gabr method, etc. The proposed design methods can be used to calculate the tensile forces in the geo-grids generated by self-weight of the different layers; wheel load of heavy vehicles; membrane effect at the base (or subbase) subgrade interface. It is then possible to set the number and the mechanical characteristics of geo-grid layers required for absorbing the horizontal forces generated by these three mechanisms.

In recent years, many designers and leading geo-grid manufacturers favour the use of a parameter called layer coefficient ratio (LCR) to quantify the benefits of geo-grid reinforcement into pavement design. This approach is sensible and more technically correct. The LCR approach applies and limits the geo-synthetic benefit derived from trials to the specific layer improved by inclusion of reinforcement (granular base course layer) whereas the TBR approach applies to the whole pavement section. Therefore, extrapolation of TBRs derived from a limited set of trafficking trials to general pavement design may or may not be valid. On the other hand, the limited focus of the LCR is more robust, Table 4.2 summarizes the various studies performed by the researchers on pavement design methodologies adopting geo-synthetics. Figures 4.1 and 4.2 shows the variation of LCR with subgrade CBRs for different tensile strengths of geo-synthetic layers. It can be found that for planar geo-synthetic reinforcements, the LCR values are ranging from 1.2 to 1.9.

Figure 4.2 Variation of LCR with subgrade CBR

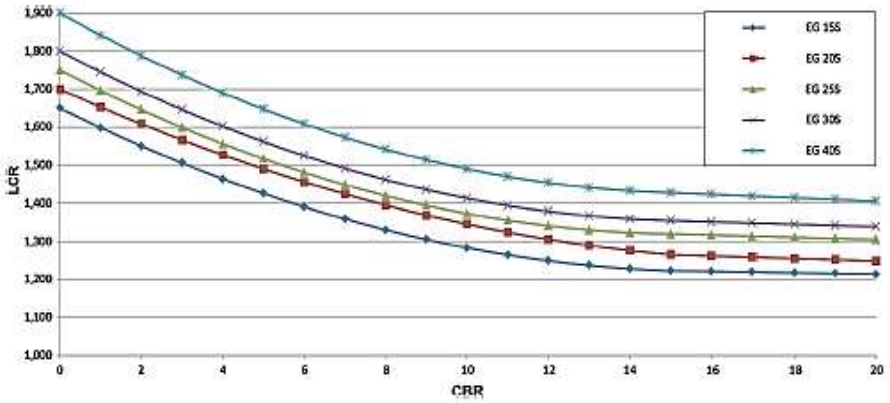

Table 4.2 Summary of studies performed on design of geo-synthetic reinforced pavements

Study	Geo-synthetics used	Remarks
Korulla et al.	Geo-grid	Given the chart of LCR with change in CBR
Technical note	Geo-grid	LCR ranges from 1 to 1.9 based upon CBR

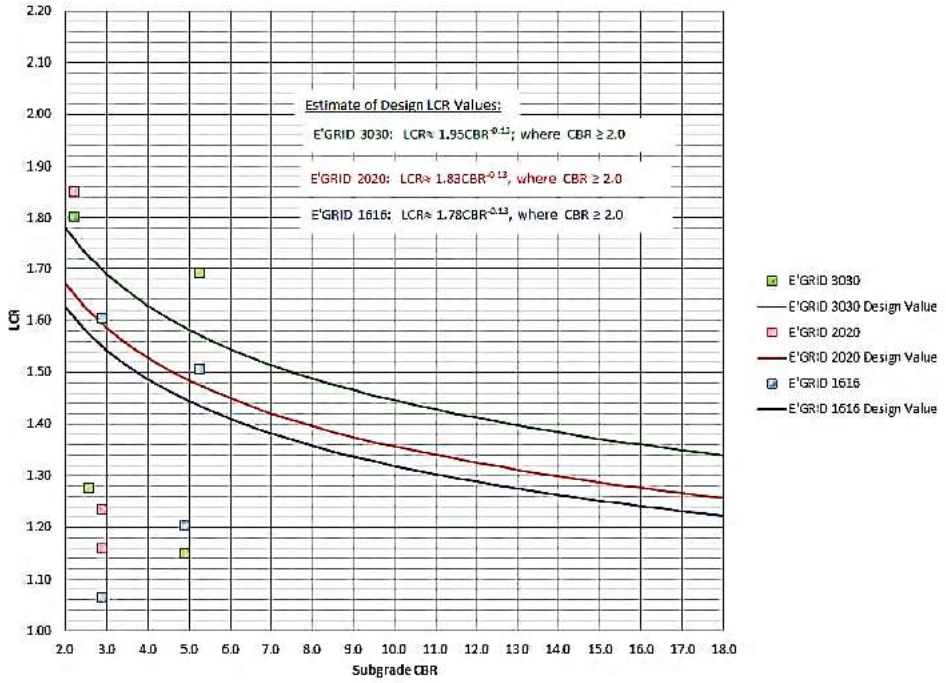

Figure 4.3 Estimate of LCR for Design based on Performance at 25 mm Permanent Deflection

As discussed in the above sections, numerous large scale laboratory studies have been conducted on unreinforced and reinforced pavement bases. The performance in terms of Traffic Benefit Ratio (TBR) and the Layer Coefficient Ratio (LCR) have been listed in the Tables 4.1 & 4.2. From these Tables, it can be noticed that the TBR & LCR have been significantly improved the performance of pavements. In India, limited studies are available on the geocell reinforced base layers on weak subgrade soils. In view of this, the current study focuses on the design of geocell reinforced pavement bases as per the IRC codal provisions and comparing it with the AASTHO specifications. Set of tests have been conducted on the unreinforced and geocell reinforced pavement sections in the laboratory and the test results have been discussed in the following chapters.

V DESIGN METHODOLOGY

The design methodology needs to address the mechanisms of pavement failure, loading intensities and also develop suitable approaches for evaluation of pavement performance. In the recent years, the use of geocells to improve pavement performance has been receiving considerable attention. This paper studies the influence of geocells on the required thickness of pavements by placing it below the granular layers (base and sub-base) and above the subgrade. The reduction in thickness here refers to the reduction in the thickness of the GSB (Granular Sub-base) layer, with a possibility of altogether getting rid of it. To facilitate the analysis, a simple linear elastic approach is used, considering six of the sections as given in the Indian Roads Congress (IRC) code. The results show that the use of geocells enables a reduction in pavement thickness.

VI. MATERIALS AND METHODS

In this Chapter, the properties of different materials used, and sample preparation techniques adopted in the present study are presented. The material properties are stated first and then the sample preparation procedures are elaborately discussed. The following materials are used in the study:

- Clayey sand to prepare a subgrade.
- Wet mix macadam (WMM) as a base course.
- Bituminous macadam as a surface layer.
- Geocell mattress as a base layer reinforcement.

The detailed characterization of each material is discussed below.

6.2 Characteristics of Subgrade Soil

The soil used for the study is natural lateritic clayey soil obtained from the Kumbakonam – Mannargudy Road at Km 8+400, Tamil Nadu.

6.2.1 Sieve analysis

A dry sieve analysis as per IS-2720 (Part4-1985) [32] was performed to determine the particle size distribution of the soil. Fig. 6.1 shows the particle size distribution of clayey soil, which consists of about 40%, fines (i.e. particles smaller than 75μ sieve size). For further classification of the soil, Atterberg's limits tests were

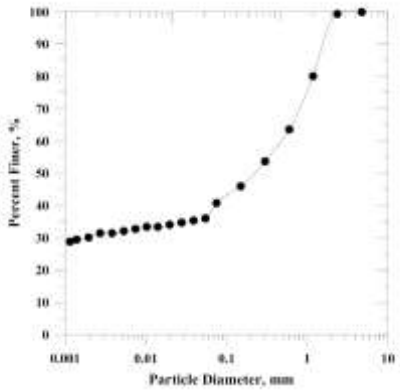

Figure 6.1 Sieve Analysis of the subgrade soil

performed.

6.2.2 Atterberg's limits

Atterberg's limits including liquid limit (LL) and plastic limit (PL) were conducted as per IS-2720 (Part4-1972). The images of apparatus used during this test can be seen in Fig.6.2, Fig. 6.3 shows the flow curve of the soil. The liquid limit and plastic limit of the soil are found out to be 47% and 21% respectively. The Plasticity Index of the soil, which is the difference between LL and PL is found out to be 26%. As per the Indian standard soil classification system, the soil is found out to be well graded sand with clay (SC).

6.2.3 Specific gravity

The specific gravity test is conducted as per IS-2720 (Part3-1980) and the specific gravity is found out to be

2.65. This test is conducted by using density bottle method.

Figure 6.2 Images of Liquid Limit and Plastic Limit

Figure 6.3 Flow Curve of Clayey soil

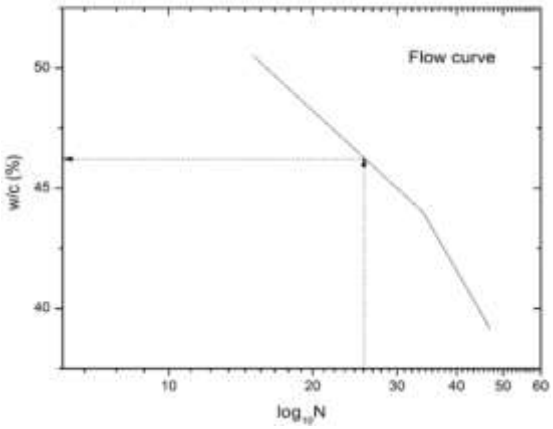

6.2.4 Compaction characteristics

The Standard Proctor compaction test is a laboratory method of finding the optimum moisture content (OMC) and maximum dry unit weight (MDU) which is conducted as per IS-2720 (Part7-1980) [35]. According to the procedure, the soil is compacted in three layers in compaction mould of volume 948 cc and each layer is given

25 blows from a standard hammer of weight 2.6 kg and falling height of 310 mm.

Figure 6.4 Mould and Hammer used in Standard Proctor Test

The images of the apparatus used during the test are shown in Fig.6.4 and the relation between unit weight and moisture content is shown in Fig.6.5. From the graph, it is inferred that the optimum moisture content (OMC) is observed as 13.9% and maximum dry unit weight (MDU) as 18.25kN/m3.

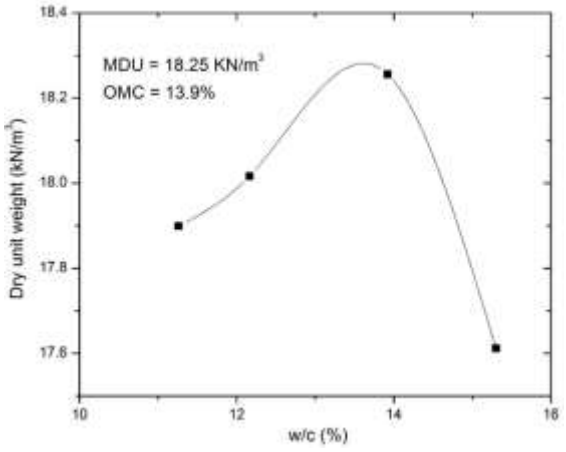

Figure 6.5 Compaction Characteristics of the subgrade soil

6.2.5 California Bearing Ratio

The California bearing ratio (CBR) test is used to determine the bearing resistance of subgrade soils. According to Indian roads congress (IRC) guidelines, the flexible pavement design is dependent on this value. This test was conducted as per IS-2720 (Part16-1987) on the subgrade clayey soil. The CBR setup is shown in Fig.6.6.

The values of the CBR in soaked and unsoaked conditions are 4.9% and 7.8%, respectively. For further analysis and the design of pavement section, CBR of about 5% was considered. The results obtained are shown in Fig.6.7.

Figure 6.6 CBR setup and post test specimen

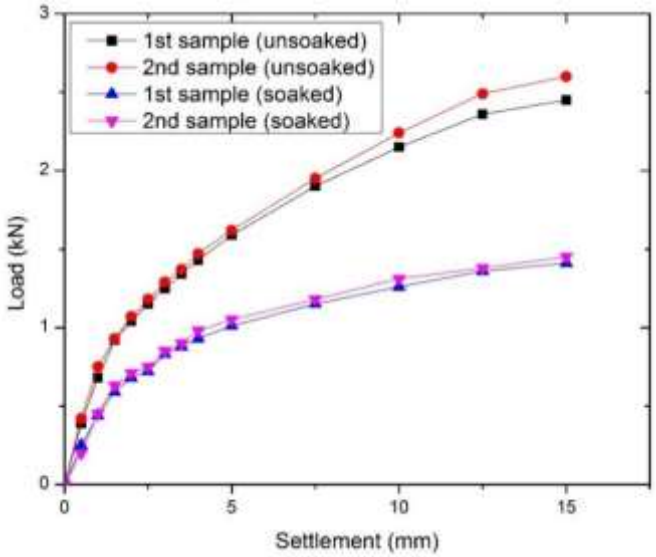

Figure 6.7 Load settlement test for CBR test

6.3 Characteristics of Wet Mix Macadam (WMM)

The wet mix macadam (WMM) is considered as per MORTH specification, 406.2.1.2. (Table 400-11) [37]. As per the MORTH, the aggregate shall conform to the grading given in Table 6.1 to be qualified as a base course material for the pavement. Aggregate material was obtained from a quarry near Sengipatti village, Thanjavur, Tamil Nadu to regrade and bin the material as per the MORTH's requirements.

Table No. 6.1 Grading requirement of aggregates for Wet Mix Macadam

IS Sieve Designation (mm)	% by weight passing the IS sieve
53	100
45	95-100
26.5	---
22.4	60-80
11.2	40-60
4.75	25-40
2.36	15-30
0.6	8-22
0.075	0-8

6.3.1 Compaction characteristics

The Modified Proctor compaction test is a laboratory method of finding the optimum moisture content (OMC) and maximum dry unit weight (MDU) which is conducted as per IS-2720 (Part8-1980). According to the procedure, the material was compacted in 5 layers in compaction mould of volume 948 cc and each layer was given 25 blows from a standard hammer of weight 4.9 kg and falling height of 450 mm. Fig 6.8 shows the variation of unit weight with moisture content. From the graph, it is inferred that the OMC is about 6.5% and MDU as about 22.48 kN/m3.

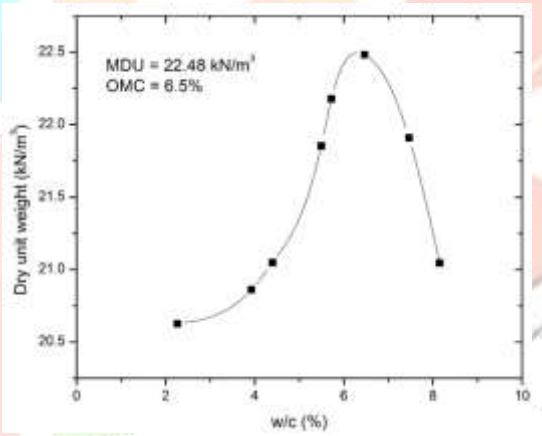

Figure 6.8 Compaction characteristics of the Wet Mix Macadam layer

6.4 Characteristics of Geocell

Geocell is a three dimensional geo-synthetic material made up of high density polyethylene (HDPE) strips, ultrasonically welded at joints, expanded on site to form a honeycombed structure. Geocell binds the infill material and also provides lateral restraint to loading. Geocell mattress used in the current study is made up of a polymer of HDPE with a density ranging from 0.935 to 0.965 gm/cm3 and a weld spacing of 356 mm.

The height or depth of the cell is maintained at 200 mm with a minimum cell strength of 2100 N throughout the test series. A typical geocell mattress used in the given study can be seen in Fig. 6.9.

Figure 6.9 Typical geocell used in the study

6.5 Characteristics of bituminous course (BC) layer

A visco-elastic bituminous concrete layer is laid as a surface course. Bitumen of Viscosity grade VG30 was used with an optimum bitumen content is 5% to 5.5%. The composition of aggregates i.e. gradation of aggregates used in the bitumen concrete is presented in Table 6.2.

IS sieve (mm)	Cumulative % by weight of total aggregate passing
26.5	100
19	79-100
13.2	59-79
9.5	52-72
4.75	35-55
2.36	28-44
1.18	20-34
0.6	15-27
0.3	10-20
0.15	5-13
0.075	2-8

Table 6.2 Grading requirement of aggregates for bitumen layer

6.6 TEST METHODOLOGY

6.6.1 Test setup

The subgrade soil was prepared and compacted at their required density and placement water content in a test tank measuring inner dimensions of 1m × 1m x 1m (length x width x height). On top of the subgrade soil a granular base layer i.e. WMM with and without geocell mattress were prepared. On the top of the base course layer a 50 mm thick layer of bituminous course was laid and compacted up to the required density. The test bed configuration and densities maintained will be discussed in the subsequent sections below. Once the final

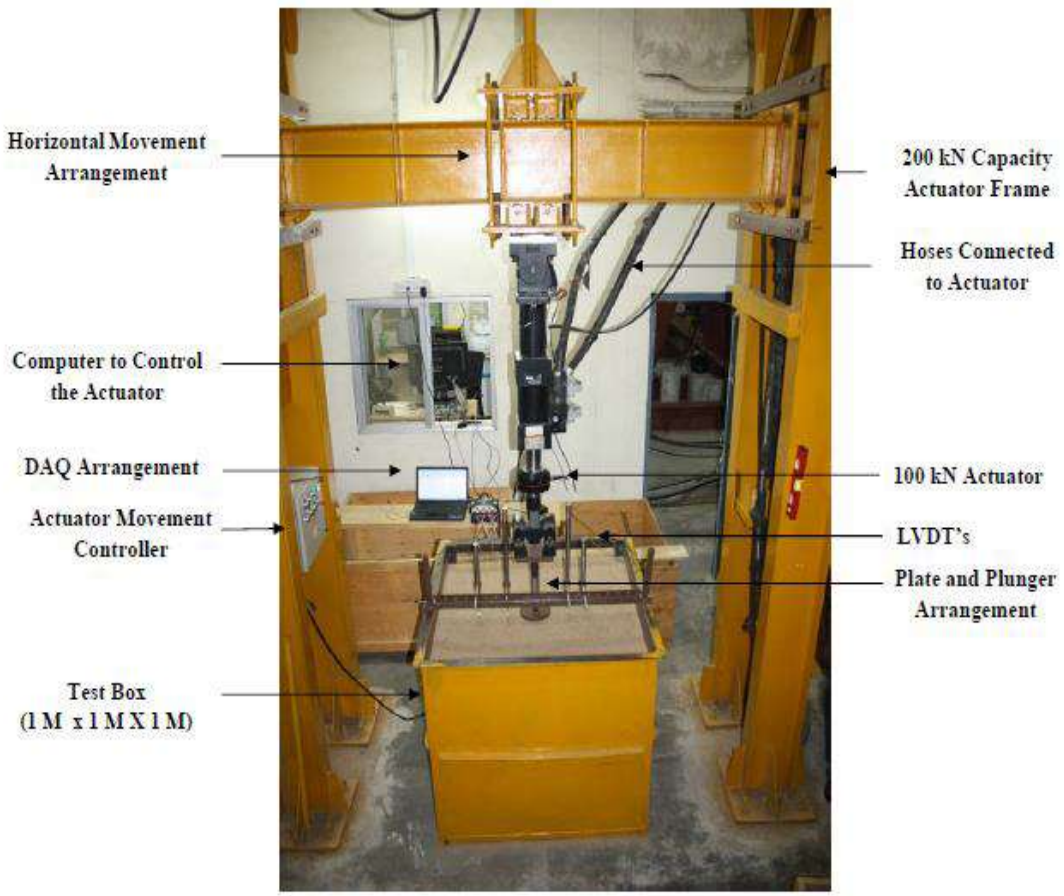

grade was prepared, a rigid thin steel plate of 150 mm diameter (D) and 15 mm thickness was concentrically placed to apply the appropriate static or repeated traffic loading. The size of the plate was chosen based on the previous experimental studies conducted in a similar testing by *Edil et al*. Loading was given by graphical user interfaced MTS MPT software with the help of hydraulic power unit (HPU), hydraulic service manifold (HSM) 34 and sophisticated double acting linear dynamic 100 kN capacity actuator which is attached to a 3.5 m high, 200 kN capacity reaction frame as shown in the below Fig. 6.10.

Figure 6.10 Large scale test setup

6.6.2 Preparation of test beds

Following are the stages adopted for the preparation of entire pavement section.

- Preparation of calibration charts.
- Preparation of subgrade.
- Preparation of base course layer.
- Preparation of bitumen course layer.

6.6.2.1 Calibration charts

To determine the number of blows required to achieve the maximum dry unit weight in the test tank, initially, a calibration test tank of size 0.6m × 0.6m × 0.6m was adopted. The pulverized soil was premixed with a required moisture content was filled in the tank with a 50 mm thick layer, which was then compacted with a hammer of weight 5kg falling from a free height 50cm on a plate size of 200mm × 200mm. The number of blows 3, 5, 7 and 9 were given in different trials, respectively, and measured the unit weights with the help of two core cutters of different sizes at every trial. A graph was then prepared to obtain the relation between the number of blows and the resultant unit weight. The calibration curve is shown in Fig. 6.11. From the graph it can be easily inferred that 8 blows are needed to achieve a required unit weight (MDU) of 18.25 kN/m^3.

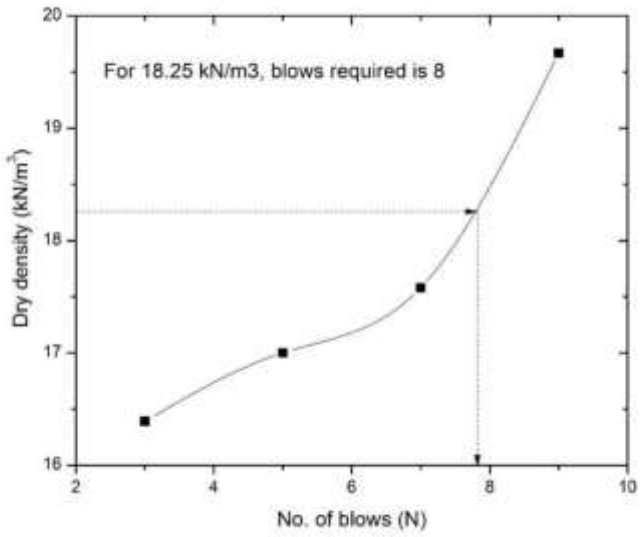

Figure 6.11 Calibration Curve for subgrade

6.6.2.2 Subgrade preparation

For the preparation of the subgrade, the soil was placed in the large test tank and compacted in 50 mm thick layers till the desired height was reached. For each layer the required amount of soil to produce a desired unit weight of 18.25 KN/m^{3}was weighted and placed in the tank. The soil was then compacted using the 5kg drop hammer to a pre-calibrated number of blows (8 blows) to achieve the required unit weight. After each layer compaction, the level was checked.

6.6.2.3 Base course preparation

To prepare the unreinforced test bed, the WMM material was placed in the test tank and compacted in 50 mm thick layers till the desired height was reached. For each layer the required amount of aggregate to produce a

desired bulk unit weight 22.48 kN/m3was weighted out and placed in the test tank making use of a metal scoop. The granular base course was then gently levelled and compacted using a vibrator. After each layer compaction, the level was checked.

For the Geocell reinforced test bed, the compaction was done using a drop hammer of weight 5 kg, height of fall 50 cm with a plate size of 100 mm × 100 mm to allow a required compaction inside the individual geocell pockets. The compaction was done to achieve a layer height of 50 mm. The level was carefully checked after each layer compaction.

6.6.2.4 Preparation of Bitumen layer

The aggregates were taken as per the grading specifications specified before, were then mixed with an optimum bitumen content of 5.2%. A layer of tack coat was first sprayed on top of the base course layer and then the bitumen mix was placed on top of the base course layer. Then the layer was compacted with the help of a drop hammer. The material was compacted till 50 mm height of layer is achieved. The size of the surface layer is kept as 800 mm × 800 mm × 50 mm. Fig. 6.12 shows the complete overview of the test section.

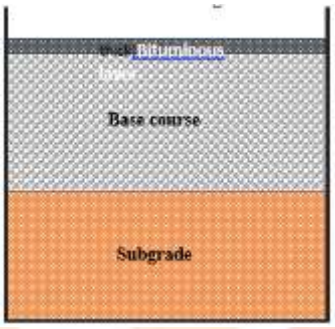

Figure 6.12 A typical section reflecting the different layers

Fig. 6.13 shows the staged preparation of test bed, the first image is of empty test tank of volume 1m^3, in the second stage the soil is compacted for the subgrade bed, the third stage is the placing of pressure cells on top of the subgrade, the fourth stage is of placing the plate rod assembly along with geocell mattress, in the fifth stage the base layer is compacted till the required density achieved, in the next stage 4 plates are used which will be placed such that the dimensions of bituminous layer should be 80mm×80mm, the tack coat is then applied on the top of the base course layer so to get a proper bond between surface layer and base layer, after spraying of the tack coat the bituminous concrete material is poured and compacted properly to achieve the levelled surface.

Figure 6.13 Various stages for the preparation of test section

6.6.3 DATA ACQUISITION SYSTEM AND INSTRUMENTATION

6.6.3.1 DATA ACQUISITION SYSTEM

Data acquisition system (DAQ) from Hottinger Baldwin Messtechnique (HBM), Germany make is used to acquire the data from all the instrumentations used in the testing. There are two types of HBM‟s Quantum X data acquisition systems used namely MX 840 and MX 1615 which are seen in Fig. 6.14.

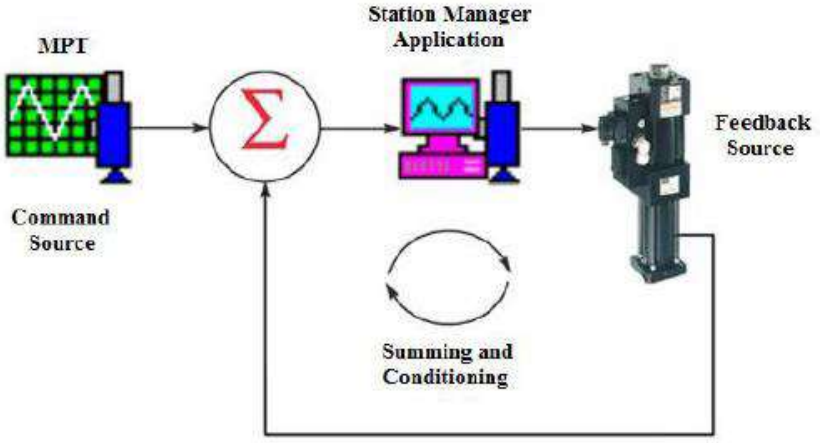

Figure 6.14 DAQ Systems MX 840 and MX 161

The MX840A is an 8-channel universal amplifier which supports all current transducer technologies and MX1615 B which is the 16-channel universal amplifier used mostly in specific to strain gauges. The DAQ‟s are connected together using a fire wire cable which comes from the manufacturer.

Then the sensors are connected to the respective DAQ's after the connection arrangement is made. The sensors are then accessed by the laptop connected to the DAQ's by giving the information of the sensor like the excitation voltage, bridge resistance, sensitivities for the range of the sensors. Sensors are then checked and verified using the sensitivities given by the manufacturer. Otherwise, they are calibrated depending on the type of the sensor.

6.6.3.2 Multi-Purpose test ware

Multi-Purpose Test ware (MPT) allows user to create complex test designs with discrete processes. Each process thus represents an individual test activity. A set of processes is grouped together in a closed loop to generate a have sine loading pattern.

The tests can be done into two ways viz. Force controlled method and Displacement controlled method. The tests done in the study were based on forced controlled method in which the configuration of devices provides a means of comparing a command signal (programmer output) to generate a signal with a feedback (transducer output) signal to generate a signal that controls a servo valve. The servo valve controls hydraulic flow of the actuator which moves the actuator piston rod. The actuator piston rod applies the force required to displace the component to be tested. Entire process is referred as "closed-loop control system" since, process of command, feedback, comparison and servo valve is a function of control circuitry and occur without operator interaction. A typical MPT close-loop control program is shown in Fig. 6.15.

Figure 6.14 Typical close loop control program in MPT software

6.6.4 Test procedure

The test procedures adopted for different types of tests are programmed using the multi-purpose test software of MTS for operating the hydraulic actuator. Upon filling the test tank up to the desired height, the fill surface was levelled, and the loading plate was placed on a predetermined alignment such that the loads from the actuator would transfer concentrically to the loading plate. To ensure this, a recess was made into the loading plate at its center to accommodate a ball bearing through which vertical loads were applied to the loading plate. The loading plate was located carefully at the center of the hydraulic actuator mounted to the reaction frame of 3.5 m height to avoid eccentric loading. The actuator was then slowly moved close to the loading plate at a very slow rate such that the plate is in contact with the actuator. Each test according to the requirement was preloaded in the software and all the settings like the acquisition rate, loading rate and the loading pattern were set, then the test command was given to execute the test with the limits given in terms of displacement or force. Each type of tests was explained in the subsequent sections. In reinforced beds, the loading plate was allowed to settle till 25mm settlement of the plate. The load transferred to the loading plate and the settlements were measured through a pre-calibrated load cell and an in line LVDT placed along the actuator. The deformations (heave/settlement) of the pavement surface on either side of the plate were also measured using LVDT's placed at a distance of 1.0D and 1.5D from the centreline on either side of the loading plate. The settlement of the subgrade was also measure though a specially designed settlement plat and a cover placed at a distance of 1.0D from the edge of the plate. The readings from the LVDT's are recorded from the HBM make MX 840 data acquisition system (DAQ) along with the testing. The pressure cells are installed on top of the subgrade at a distance 1D, 1.5D and 2D from the center line of loading plate and also at the center.

6.6.4.1 Static load tests

The static plate load tests were carried to estimate the ultimate strength for unreinforced and reinforced test sections. The test is carried out by applying a settlement or displacement rate of 0.5 mm/min. The response in terms of pressure and settlement is obtained to analyse the data further. Fig. 6.16a shows the loading pattern used in static loading test.

6.6.4.2 Repeated load tests

The repeated load test on the specimen is applied by carefully placing the plate at the center of the actuator against the reaction frame to avoid eccentric loading. Initially, the seating load was applied to a loading plate using a computer-controlled servo hydraulic actuator. The repeated load with a maximum load of 9.7 KN which is an equivalent pressure of 550 kPa (which is a typical tire pressure of a highway truck) and minimum load of 0.97 KN which is equivalent to 40 kPa is applied at a frequency of 1.0 Hz. A 10% of load (0.97 KN) was constantly applied on the plate to make the cycle a closed loop. This loading corresponds to the pressure transmitted on to the subgrade. Multi-Purpose Test Ware (MPT) software was set up to control and acquire the applied load data as well as the deformation data. The loading pattern adopted in this study can be seen in Fig. 6.16b.

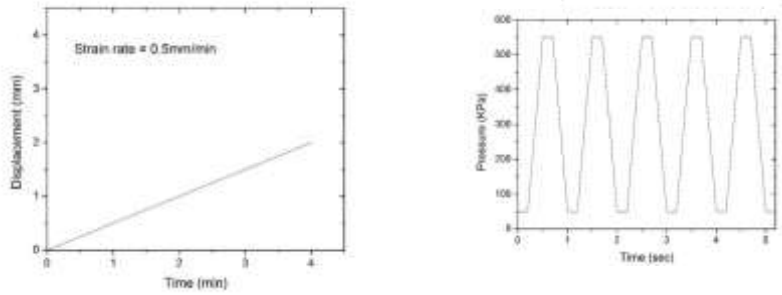

(a) (b)

Figure 6.16 Typical loading patterns (a) for static test (b) repeated load test

6.7 PERFORMANCE INDICATORS

Several performance indicators are introduced to evaluate the efficacy of each reinforced test configuration over its counter unreinforced bed. These parameters are presented in the following sections.

6.7.1 Cumulative permanent deformations

To analyse the data in terms of permanent deformations (or rutting), the total settlement accumulated from each cycle has been split up in to two components viz. elastic and plastic settlements as shown in Fig. 6.16.

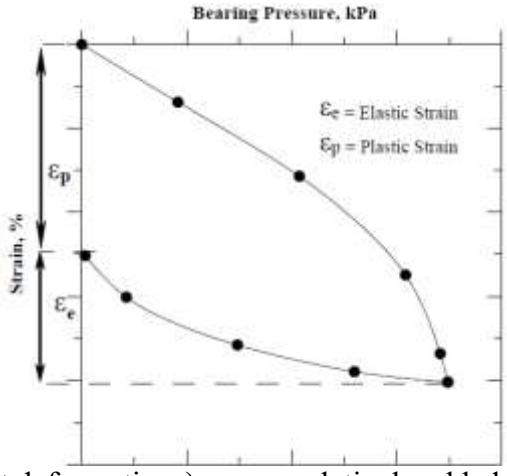

The plastic settlements (permanent deformations) are cumulatively added to obtain the cumulative permanent deformations (CPD).

Figure 6.17 Elastic and plastic strains of a typical loading cycle

6.7.2 Traffic benefit ratio

To quantify the benefits from the geo-synthetics especially in pavement applications, a non-dimensional term has been introduced and is expressed in terms of extension of life or by savings in base course thickness. Extension of life is defined in terms of a Traffic Benefit Ratio (TBR). TBR is defined as the ratio of the number of load repetitions necessary to reach a given rut depth for a test section containing reinforcement, divided by the number of repetitions necessary to reach the same rut depth for an unreinforced section with the same section thickness and subgrade properties. The following is a mathematical expression for TBR evaluation.

$$TBR = \frac{N_r}{N_u} \qquad \text{..... } 6.1$$

where, N_r = No. of cycles required to reach given amount of rut depth

N_u= No. of cycles required to reach same amount of rut depth

6.7.3 Rut depth reduction

To quantify the rutting behaviour of geocell reinforcement, a parameter rut depth reduction (RDR), expressed in percentage, for different cases is introduced. RDR can be defined as the ratio of difference between cumulative permanent deformations of the unreinforced bed ($CPD_{unreinf}$) and geocell reinforced bed (CPD_{reinf})

$$(RDR)_N = \left(1 - \frac{CPD_{reinf}}{CPD_{unreinf}}\right) \times 100 \qquad \text{.... } 6.2$$

to that of the unreinforced bed for a particular number of loading cycle. Hence, RDR for an n^{th} load cycle can be expressed as:

6.7.4 Equivalent modulus improvement factor

Equivalent modulus improvement factor (EMIF) is a ratio of total elastic modulus of reinforced test section (E_r) to the total elastic modulus of the unreinforced test section (E_u) with the same test configuration. The equivalent modulus improvement factor is introduced to quantify the effect of geocell reinforcement in the pavement test section. This parameter is very important in analysing the pavement sections and their design.

$$\text{EMIF} = \frac{E_{reinf}}{E_{unreinf}} \qquad \text{....6.3}$$

6.7.5 Rut benefit ratio

To quantify the rutting behaviour of geocell reinforcement at the subgrade level, a parameter known as rut benefit ratio (RBR), expressed in percentage, for different cases is introduced. RBR can be defined as the ratio of difference between cumulative permanent deformations of the unreinforced bed ($CPD_{unreinf}$) and geocell reinforced bed (CPD_{reinf}) to that of the unreinforced bed for a particular number of loading cycle. However,

$$(RBR)_N = \left(1 - \frac{CPD_{reinf}}{CPD_{unreinf}}\right) \times 100 \quad \text{....6.4}$$

CPDs are precisely measured on the subgrade surface. Hence, RBR for an nth load cycle can be expressed as:

6.7.6 Layer coefficient ratio

Layer coefficient ratio (LCR) is defined as the ratio of layer coefficients of reinforced to that of unreinforced layer. It is a measure of improved structural capacity of the reinforced pavement layer. While reinforcing base

$$LCR = \frac{0.249\ log_{10}(EMIF.M_{r2}/0.0069) - 0.977}{0.249 log_{10}(M_{r2}/0.0069) - 0.977} \quad \text{....6.5}$$

layers, it is calculated as:

where, M_{r2} = Resilient modulus of base course layer

Overall, a detailed experimental program has been evaluated and discussed all the methods to be adopted and materials to be used in this chapter to design a real pavement section for a known CBR value of the subgrade.

VII RESULTS AND DISCUSSION

In this chapter, the pavement test sections were designed according to the IRC37-2012 guidelines based on the material properties (CBR=5%). The design pavement test sections with and without geocell reinforced base layers were tested by applying a static load at a uniform displacement rate of 0.5 mm/min. Further, based on the equivalent modulus improvement factor obtained from the pressure-settlement curves, the geocell reinforced test sections were re-designed with a reduced base thickness. As mentioned in the previous chapter, the proposed methodology is followed to carry out the large scale testing program. The static and repeated load tests performed on these test sections are discussed in detail along with the design approach involved in the following sections.

7.2 DESIGN APPROACH

The flexible pavements are designed as a layered system in which the wheel loads are transferred to the lower layers by distributing the loads to a wider area. The stresses and strains at critical locations are computed using linear elastic models. The pavements should be designed such that they should perform efficiently throughout their design life. The failure of flexible pavements is generally due to fatigue cracking and the formation of ruts, which can be visualized on the pavement surface.

(i) Vertical compressive strain at the top of the sub-grade which can cause sub-grade deformation resulting in permanent deformation at the pavement surface.

(ii) Horizontal tensile strain or stress at the bottom of the bituminous layer which can cause fracture of the bituminous layer.

The design methodology (as per IRC 37-2012) adopted in the current study is discussed in the following steps.

Step 1. Finding the allowable fatigue and rutting strains at critical locations.

Fatigue strain is the horizontal tensile strain (Ɛt) at the bottom of the bituminous bound layer, which is an indicator for fatigue cracking in the bituminous layer. Rutting strain is the vertical strain on top of the subgrade (Ɛv), which is considered to be causative factor for permanent deformation in subgrade (Fig. 7.1). The allowable fatigue and rutting strains are computed from the following models specified in IRC 37-2012.

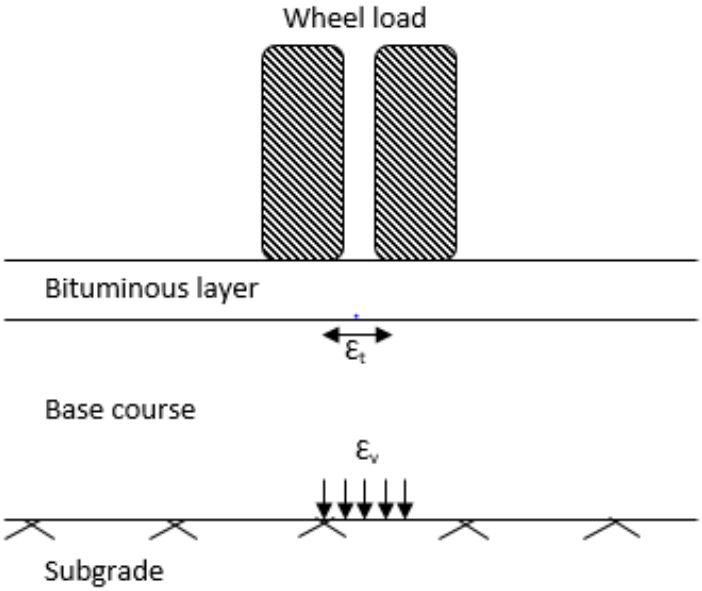

Figure 7.1 Locations of critical strains

Fatigue equation for 90% reliability is given as:

$$N_f = 0.711\times10^{-4}\times\left(1/\varepsilon_t\right)^{3.89}\times\left(1/M_R\right)^{0.854} \quad \text{..... 7.1}$$

where, N_f = fatigue life in number of cycles

ε_t= Maximum tensile strain at the bottom of bituminous layer

M_r= Resilient modulus of bituminous layer

Rutting equation for 90% reliability is given as:

$$N_f = 1.41\times10^{-8}\times\left(1/\varepsilon_v\right)^{4.5337} \quad \text{.....7.2}$$

Where, N = Number of cumulative standard axles

ε_v= Vertical strain in subgrade

Step 2. Selecting an appropriate thickness of pavement layers from the design charts (CBR Plates)

Thickness of the pavement layers are computed from the design catalogues given in IRC for relevant traffic and subgrade conditions.

Step 3. Finding the fatigue and rutting strains using IITPAVE

As discussed earlier, IITPAVE, a computer program developed by IIT Kharagpur is used to find out the strains at the critical locations as shown in Fig. 7.1. Incorporating the above trial thickness in the IITPAVE software, fatigue and rutting strains for the selected pavement section are computed and are verified against the allowable strains.

Step 4. Arriving at the final thickness

For a safe and efficient pavement system, the fatigue and rutting strains (obtained in step 3) should be less than the limiting fatigue and rutting strains (obtained in step 1). If the strains obtained are less than the limiting strains, the selected pavement section thicknesses can be adopted.

Based on the above design procedure, for a subgrade soil CBR of 5% and a traffic equivalent to 2 msa, the CBR plate shown in Fig. 7.2 is referred to obtain the design pavement section thicknesses. The pavement

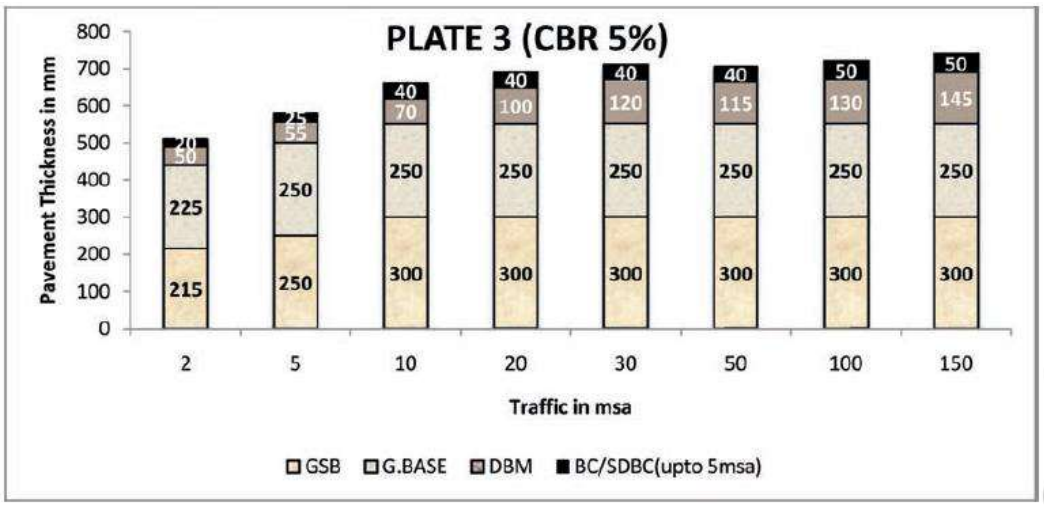

thickness corresponding to the subgrade condition and the expected traffic flow are provided in the design catalogues of IRC 37:2012.

Figure 7.2 Typical pavement design chart for subgrade CBR of 5% (IRC 37:2012)

From Fig. 7.2, as per the subgrade and traffic conditions mentioned above, a pavement test section with a total thickness of 510mm was obtained. The pavement section consists of a 215mm granular sub-base layer, 225mm granular base layer, 50mm thick dense bituminous macadam and a 20mm thick bituminous concrete layer. However, as per the design steps explained above, the total thickness of the pavement section is found to be 490mm comprising of 440mm of granular base and sub-base layers and a 50mm thick bituminous concrete layer.

7.2.1 Verifying the results of IRC using AASHTO (1993)

The thicknesses and the properties of the pavement layers provided in Table 4.1 were incorporated in the AASHTO (1993) design equations and it was witnessed that the number of repetitions were reduced to 0.66msa in place of 2 msa, obtained from IRC charts. This observation suggests that, either the IRC is under predicting the pavement layer thicknesses or over predicting the expected traffic flow.

Table 7.1 Results from AASHTO method

Input Parameters	Results
E_{AC} = 435113 psi	SN_u = 3.06 W_{18} = 0.66 msa
E_B = 22336 psi	
M_R = 7252 psi	
Z_R = -1.282 psi	
S_o = 0.45	
ΔPSI = 2.3	

Table 7.2 provides the comparison of results obtained from both the IRC and AASHTO pavement design methodologies and it can be inferred that the correlations used to calculate the M_R of base layer in IRC method is inappropriate, because the IRC method considers subgrade CBR to calculate the base layer M_R.

Table 7.2 Comparison of the results

M_R= 154 MPa		M_R= 200 MPa	
IRC		AASHTO	
Traffic = 2 msa	S_{NU} = 3.06	Traffic = 2 msa	Traffic = 2 msa
CBR = 5%	D 2 = 440 mm	SNU = 3.65	SNU = 3.65
D_2 = 440 mm	Traffic = 0.67 msa	D_2 = 553 mm	D_2 = 439 mm

7.2.2 AASHTO design method through TBR approach (reinforced pavement section)

Step1: The structural number (SN) is calculated for the unreinforced test section by using the following equation.

$$SNu = a_1D_1 + a_2D_2m_2 \quad \ldots(7.3)$$

Where, SNu = structural number for unreinforced case

a_1 = Layer coefficient for surface layer and is calculated using the following equation

$$a_1 = 0.171 (\ln (E_{AC}) - 1.784) \quad \ldots(7.4)$$

d_1 = thickness of asphalt layer (mm)

a_2 = layer coefficient for granular base layer and is calculated the below equation

$$a_2 = 0.249 (\log10 (E_{BC})) - 0.977 \quad \ldots(7.5)$$

d_2 = thickness of base course layer (mm)

m_2 = drainage coefficient for base layer

E_{AC} = modulus of elasticity of asphalt layer

E_{BC} = modulus of elasticity of base layer

Step 2: By using the TBR value calculated from the repeated loading test, the designed traffic (in msa) is multiplied with TBR to get the value of modified traffic value (in msa) for the reinforced pavement section.

Step 3: The structural number (S_N) is calculated for reinforced test section by using the equation written below. The value of traffic substitute in the following equation should be the modified one.

$$Log10(W18) = ZR\ So + 9.36log10\ (SNR+1) – 0.20 + 2.32log10Mr-8.07 \quad \ldots(7.6)$$

Where, W_{18} = predicted number of 18-kip (80-kN) ESALs

Z_R = standard normal deviate (dimensionless)

So = combined standard error of the traffic prediction and performance prediction (dimensionless), 0.45 commonly used

ΔPSI = difference between the initial present serviceability index (P0) and the design terminal pavement serviceability index (Pt)

S_N = structural number of reinforced pavement layer

M_r= resilient modulus of roadbed (MPa)

Step 4: The SNR is then subtracted with S_{Nu} to get the value which is virtually inducing due to the inclusion of

the geocell in the basal layer.

Step 5: Keeping the S_{Nu} constant and by changing the values of d_2 in eq. (7.3) the structural number is then find out which is further added with the value induced due to reinforcement in the pavement section. If the value of S_{Nu} matches with equivalent structural number calculated as discussed above, then the corresponding d_2 is the revised thickness of the base course layer in reinforced case which is equivalent to the earlier thickness of the unreinforced section.

Table 7.3 Reinforced pavement design

Input parameters		Results
E_{AC} = 435113 psi		
E_{Br} = 37710psi		
M_r= 7252psi		SN_u = 3.65
Z_R	= -1.282	TBR =3.5
So	= 0.45	$(D2)_U$ =440 mm
ΔPSI = 2.3		$(D2)_R$ = 271 mm
TBR = 3.5		
W_{18} = 2msa		

7.2.3 AASHTO design through LCR approach (reinforced pavement section)

$$LCR = \frac{0.249\ log_{10}(EMIF.M_{r2}/0.0069) - 0.977}{0.249 log_{10}(M_{r2}/0.0069) - 0.977} \quad \ldots 7.7$$

$$(D_2)_R = \frac{SN - a_1 D_1}{LCR a_2 m_2} \quad \ldots 7.8$$

Where, D2(R) = Thickness of base layer in mm

Further, as per the test section designed, a subgrade of 410mm was compacted in 8 layers each of around 50mm thick and the base course layer was compacted in 9 layers each of about 50mm thick. A bituminous concrete of 50mm thickness was then compacted after the application of tack coat on the dry base course.

The static load tests were performed on the unreinforced and geocell reinforced test sections with a base course thickness of 440 mm to understand the influence of geocell reinforcement in improving the modulus of the base course layer, which in turn improves the performance of entire pavement system. The equivalent modulus improvement factor (EMIF) is estimated with the help of these static load tests performed and the detailed procedure is explained in the following section.

7.3 EQUIVALENT MODULUS IMPROVEMENT FACTOR

To determine the equivalent modulus improvement factor (EMIF), static load tests were performed on the

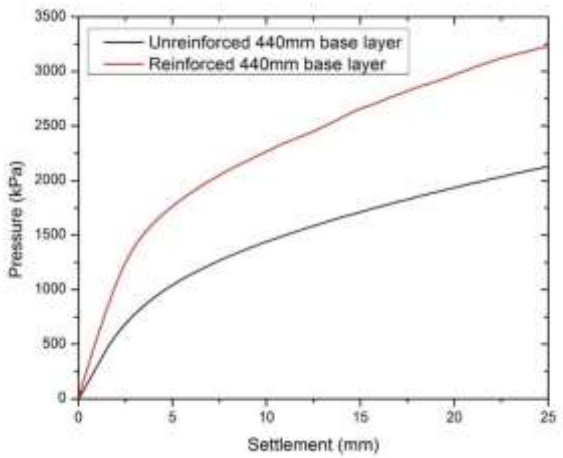

unreinforced and the geocell reinforced pavement test sections obtained as per the design approach adopted. The static load test results are obtained in the form of pressure-settlement curves for the unreinforced and geocell reinforced test sections separately as presented in Fig. 7.3. From Fig. 7.3, it can be observed that the bearing pressure in the reinforced test section is as high as 3200kPa at 25 mm settlement. Whereas the bearing pressure in the case of unreinforced test section at the same settlement (25 mm) is observed to be 2130 kPa. This observation suggests the fact that the presence of geocell reinforcement has improved the bearing pressure by almost 1.5 times the control section at 25mm settlement.

Figure 7.3 Pressure-settlement curve for 440mm thick base geocell reinforced and unreinforced test sections

The elastic modulus is calculated from the linear or elastic region of the stress-strain plots obtained for both the reinforced and unreinforced test sections. The elastic modulus obtained in both the cases are the equivalent module of the entire pavement test section, as the stress-strain curves are plotted for the static load test results obtained from the unreinforced and reinforced test sections. The EMIF can be defined as the ratio of elastic modulus of reinforced section to the elastic modulus of the unreinforced section. An EMIF of about 2.24 is achieved in the geocell reinforced test sections against the control test section. Hence, it can be inferred that the presence of geocell reinforcement has improved the stiffness of the base course layer.

Further, in geocell reinforced base layer, to maintain the same stiffness as that of unreinforced test sections, the thickness of geocell reinforced base layers can be reduced in such a way that an EMIF greater than 1 should be maintained. Hence, the base course thickness of reinforced test section was reduced from 440 mm to 250 mm and static load tests were performed on the test sections with reduce thickness. The tests were performed on the sections with reduced thickness to verify whether the EMIF value obtained is greater than 1. An EMIF of 1.3 was obtained for the geocell reinforced reduced base course thickness.

The experimental program is briefly divided into two stages as shown in Table 7.4

Table 7.4 Test summary

Stage	Test program	Configuration
1	Static load test	Unreinforced test section having 440 mm thick base course Reinforced test section having 440/250 mm thick base course
2	Repeated load test	Unreinforced test section having 440 mm thick base course Reinforced test section having 250 mm thick base course

7.4 Static Load Test Results

During the first stage, the static load tests were performed on the unreinforced test section having a 440mm thick base course (Fig. 7.4) and a geocell reinforced test section having a 250mm thick base course (Fig. 7.5) to understand the influence of geocell reinforcement in improving the base layer stiffness and also to study the performance of geocell under static load conditions. The loads were applied on the test sections at a constant settlement rate of 0.5mm/min until a settlement of about 25mm is reached and the corresponding load applied are noted. The pressure-settlement curves obtained for the test sections shown in Figs. 7.4 and 7.5 are as presented in Fig. 7.6. From Fig. 7.6, it can be observed that for the same level of settlement the reinforced section is bearing more pressure than the unreinforced one. For instance, at 5mm settlement, the bearing pressure in unreinforced case is 900kPa, whereas it is 1200kPa in reinforced case. Similarly, at 25mm settlement, the bearing pressure in unreinforced section is 2130kPa as compared to 2330kPa in reinforced section. So, at 25mm settlement a percentage increase of about 9.39% in bearing pressure is observed in reinforced case.

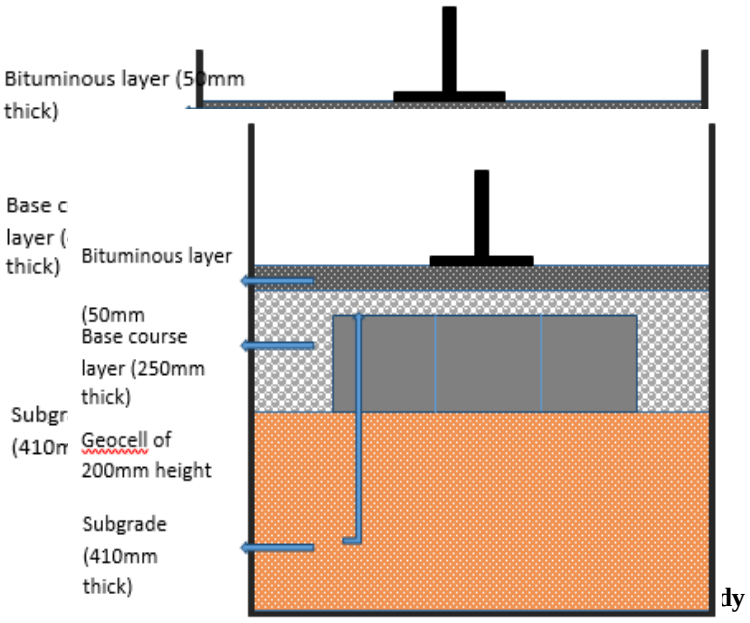

Figure 7.5 Reinforced test section used in the study

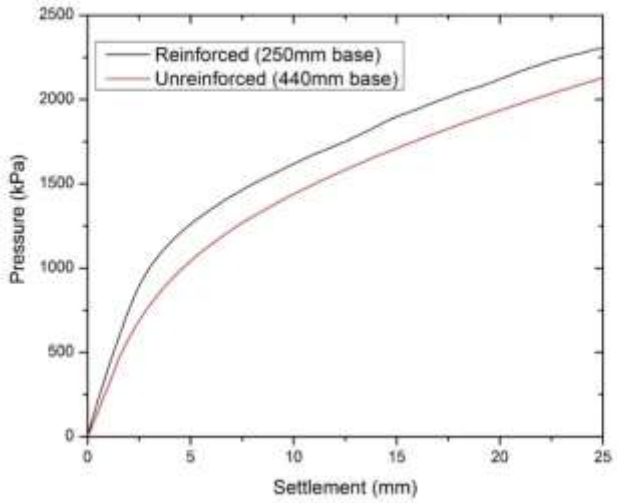

Figure 7.6 Pressure-settlement curve for 440mm thick unreinforced and 250mm thick base geocell reinforced test sections

The surface deformations and the deformation profile for both unreinforced and geocell reinforced test sections were obtained with the help of the displacement sensors located in the actuator and also the LVDTs placed at a distance of 1D and 1.5D on either side from the centreline of loading point as explained in section 6.6.4. Figure 7.7 presents the deformation profile for the unreinforced test section in the form of deflection

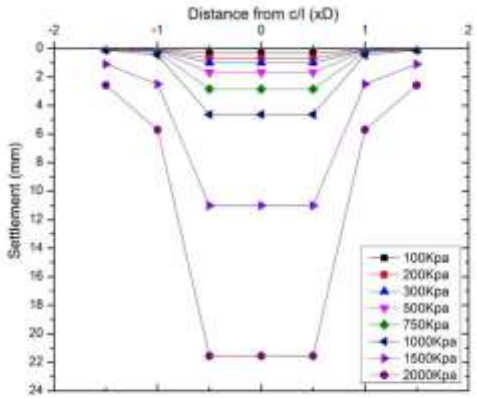

Figure 7.7 Surface deformation profile of unreinforced test section

basins. The term deflection basin can be defined as the area of pavement deflection under and near the loading region. It can be observed from Fig. 7.7 that with the increase in the pressure applied, the deflection basin gets deeper i.e. the settlement is high. However, the settlement is mainly observed below the loading region and the settlements are observed to be very less to negligible on either side of the loading region. For Instance, at an applied pressure of 1500 kPa, the settlement of the loading plate is as high as 11mm whereas, the settlements on either side of loading plate are observed to be 2 mm and 1 mm at a distance of 1D and 1.5D from centreline respectively.

Similarly, Fig. 7.8 presents the deformation profile of the geocell reinforced test section in the form of deflection basins. It can be observed from Figs 7.7 and 7.8 that for the same amount of pressure applied, the geocell reinforced section has restricted the settlement reasonably. It can also be observed from Fig. 7.7 and Fig. 7.8 that, the settlements in both the test sections are almost similar up to a pressure of 300kPa is applied. Further, with the increase in applied pressure, the settlements in the unreinforced sections have increased drastically

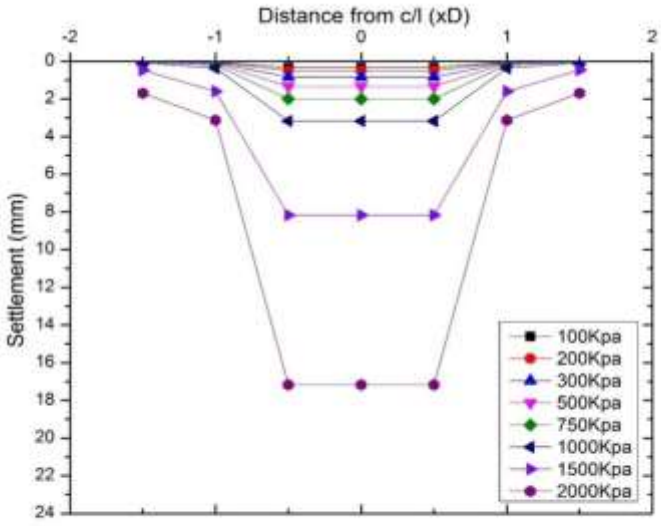

Figure 7.8 Surface deformation profile of reinforced test section (250mm base)

compared to the geocell reinforced section. From this observation, it can be inferred that the presence of geocell reinforcement in the base layer has improved the stiffness of the base layer and in turn has reduced the surface settlements of the test section.

The test sections were also instrumented with the pressure cells located at the subgrade level exactly below the loading region and at a relative distance of 1D, 1.5D and 2D from the centreline of the loading region as explained in the section 6.6.4. The pressure acting on the subgrade due to the various intensities of load applied on the surface of the test sections can be determined with the help of this instrumentation arrangement and both the unreinforced and geocell reinforced test sections were instrumented to understand the pressure distribution patterns in the pavement system. Figure 7.9 presents the pressure distribution patterns at the subgrade levels for various intensities of pressure applied on an unreinforced test section. It can be observed that, with the increase in the applied pressure, there is an increase in the pressure acting on the subgrade. The pressure distribution curve gets sharper with an increase in applied pressure i.e. the pressure recorded exactly below the loading region is high. However, the pressure acting at a distance of 1.5D and 2D are relatively less.

Similarly, Fig. 7.10 presents the pressure distribution pattern at the subgrade level for various intensities of load applied on the geocell reinforced test section. It can be observed that there is an increase in the pressure intensities recorded with an increase in the applied pressure. However, the pressure distribution patterns in the reinforced section are observed to be less narrow, unlike the pressure distribution patterns of unreinforced section.

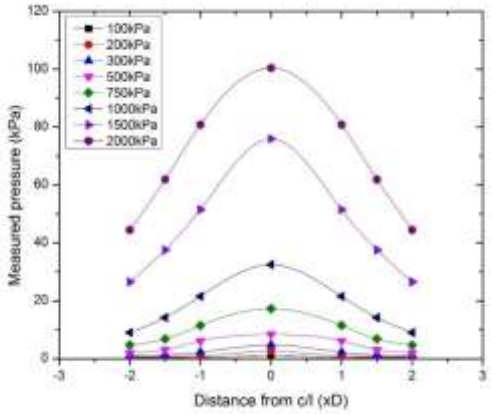

Figure 7.9 Pressure acting on the subgrade at different loads applied (Unreinforced)

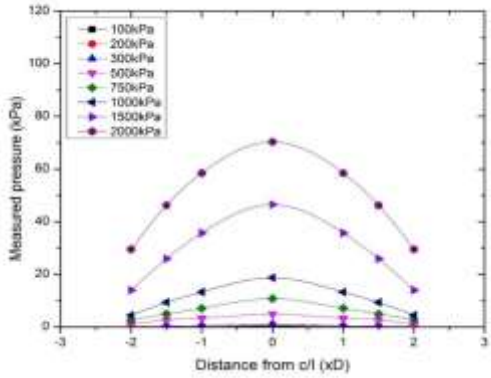

Figure 7.10 Pressure acting on the subgrade at different loads applied (Reinforced 250 mm base)

From the Fig. 7.9 and Fig. 7.10, it can be visualized that the pressure experienced at the subgrade level at all the specified locations is less in reinforced pavement section than the unreinforced section. It indicates that the geocell reinforcement is capable of distributing the loads to a wider area which in turn helps in reducing the pressure intensities observed at the subgrade level. About a 30% reduction in the pressure was observed in the geocell reinforced test sections compared to the unreinforced test sections at an applied pressure of 2000 kPa.

7.5 Repetitive Load Test Results

During the second stage, repeated load tests were performed on the unreinforced and geocell reinforced test sections as listed in Table 7.5. The repeated loads are applied in such a way that it replicates the live traffic condition in the laboratory i.e. a traffic load equivalent to a contact pressure of 550kPa. The performance of geocell reinforced test sections were compared w.r.t the control section and the performance indicators such as traffic benefit ratio (TBR), rut depth reduction (RDR), cumulative permanent deformations (CPD) and rut benefit ratio (RBR) were estimated for the geocell reinforced test sections.

In a repeated load test, there are two types of settlements observed in the pavement section i.e. elastic settlement which is ultimately regained on unloading and the other one is plastic settlement which cannot be regained, also called as permanent settlement. The summation of these plastic settlements after each loading cycle is called as cumulative plastic deformation (CPD). The variation of CPD with number of load cycles is presented in Fig. 7.11. Initially, it is observed that both the pavements are behaving same till 1000 load cycles, however, as the cycle number increases the difference in settlement increases between the two test sections.

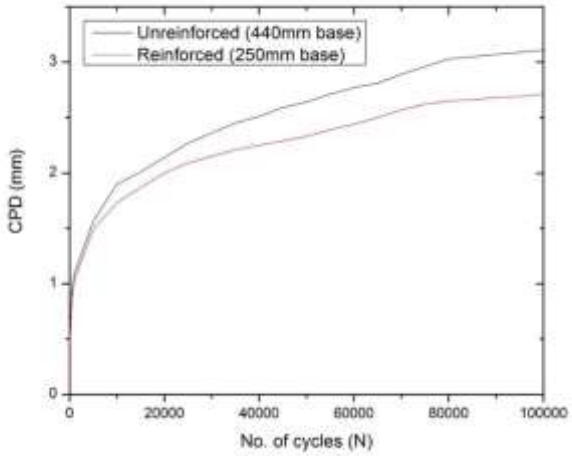

Figure 7.11 Variation of cumulative plastic deformations with no. of load repetitions

At 20,000 cycles, the deformation observed in unreinforced pavement section is around 2 mm with respect to the 1.85 mm deformation in reinforced case. At 1,00,000 cycles the reinforced pavement section settles only 2.71 mm compared to 3.11 mm in unreinforced case.

To quantify the amount of improvement, non-dimensional terms are used such as traffic benefit ratio (TBR), rut depth reduction ratio (RDR) and rut benefit ratio (RBR) graphs of which are shown in Fig.7.12, 7.13 and 7.14, respectively.

7.5.1 Traffic benefit ratio

Figure 7.12 shows variation of TBR with respect to CPD. As mentioned in section 6.7.2, the traffic benefit ratio (TBR) is a non-dimensional term used to quantify the benefits of the geo-synthetics used in pavement. It directly relates with the extension of life and also with savings in height of the base layer. As higher is the TBR value more will be its life. From the above Fig. 7.12, it is clearly seen that the TBR is increasing with the increase in CPD. A TBR of 1.7 indicates that the reinforced section will withstand till 1.7 times of designed load repetitions for unreinforced case i.e. 3.4msa in reinforced case at the same amount of settlement.

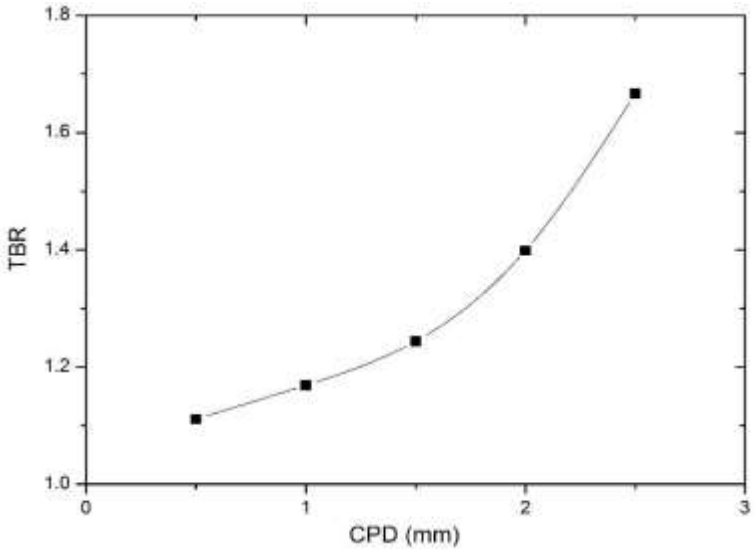

Figure 7.12 Variation of TBR with CPD

7.5.2 Rut depth reduction

It is a parameter used to quantify the pavement performance in terms of reduction in rut depth. From Fig. 7.13, it can be seen that initially the curve is steeper which changed to flattened after 80000 load cycles, it means that the reduction rate is higher initially and keeps on decreasing as the increase in number of loading cycles. It is a term which directly quantifies the reduction in rut by introducing the geocells in base layer. The rut depth reduction (RDR) is observed to be around 13% after the inclusion of the geocell in base layer, which means that the geocell helps in reducing the rut which ultimately helps in maintaining the evenness in level at top indicates good quality surface in reinforced roads.

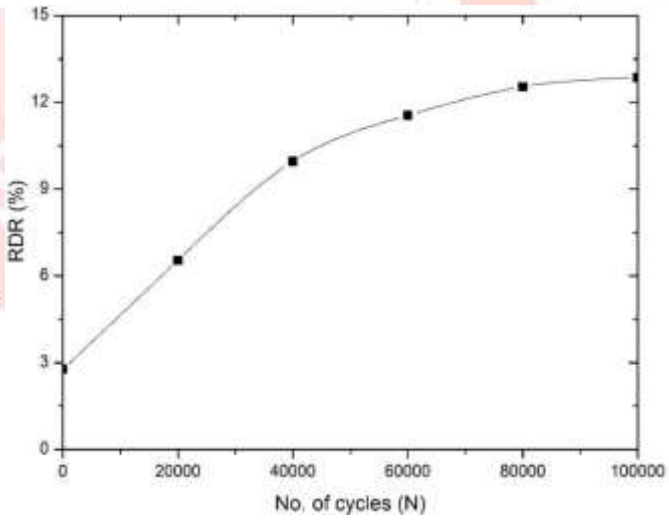

Figure 7.13 Variation of RDR with number of loading cycles

7.5.3 Subgrade deformation

The subgrade deformation results in the deformation of layers above including the surface layer, forming a rut under the traffic wheel loads. To record the subgrade deformations and to understand the actual rut behaviour at the subgrade level, an assembly consisting of two metal plates and a steel pipe is employed. The subgrade deformations recorded at different number of load cycles in both unreinforced and geocell reinforced test sections have been presented in Fig. 7.14. It can be observed that the geocell reinforced test sections have a less rut depth compared to the unreinforced test section at the same load cycles. It can be inferred that the

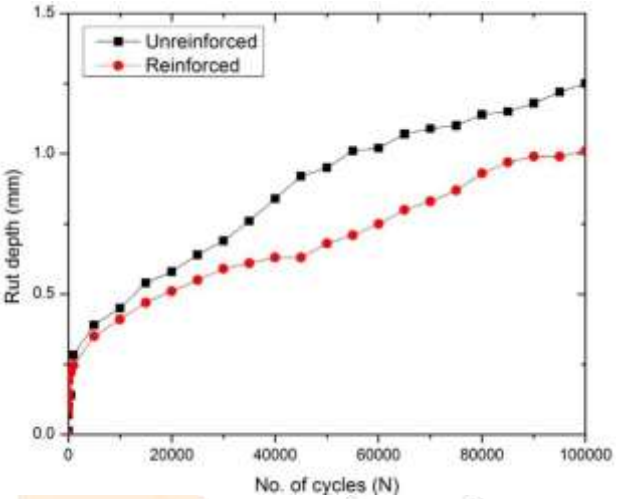

Figure 7.14 Variation of rut depth with number of load cycles

geocell reinforcement in the base layers have reduced the rut depth at the subgrade level effectively. Further, the benefit in rut depth reductions is explained in the following section.

7.5.4 Rut benefit Ratio

In this study, the rut benefit ratio (RBR) is used to evaluate the improvements in rut depth reductions at the subgrade level. The RBR is similar to the rut depth reduction (RDR) as both quantify the reduction in rutting. However, the key difference is that the RBR provides information about the rut directly at the subgrade, whereas the RDR shows improvements at the surface level. The rut benefit ratio can be as high as 20% in reinforced test sections, as illustrated in Fig. 7.15.

As discussed in section 7.3, the test sections were instrumented with linear variable differential transformers (LVDTs) and earth pressure cells for repetitive load tests. The instrumentation results were analyzed to understand the surface deformation profile and the vertical stress acting on the subgrade at different load cycles. Figures 7.16 and 7.17 present the surface deformation profiles for unreinforced and reinforced cases, respectively. Up to 1000 cycles, both profiles behave similarly, but with an increase in load cycles, the unreinforced case shows more surface settlement. It is also observed that deformation is minimal at the farthest location from the loading area compared to the line of load application. The deflection basin in the geocell-reinforced test section is s ess of the layer where it is introduced.

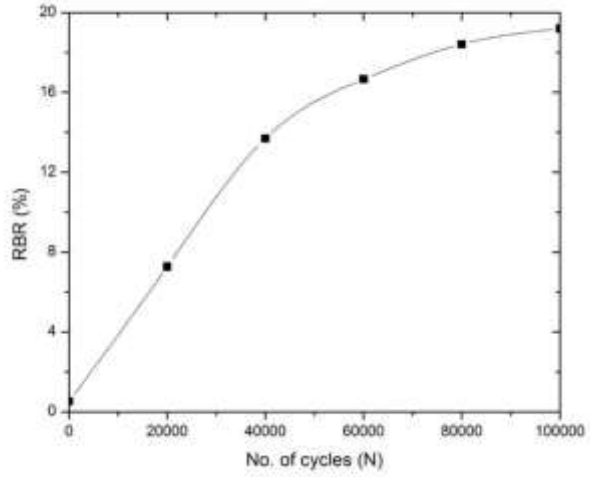

Figure 7.15 Variation of RBR with number of cycles

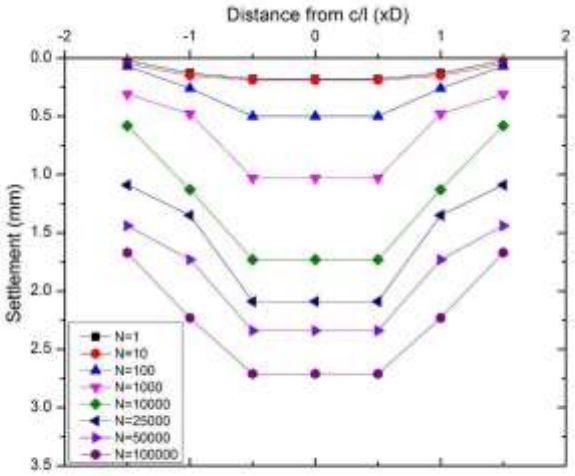

Figure 7.16 Surface deformation profile for unreinforced case

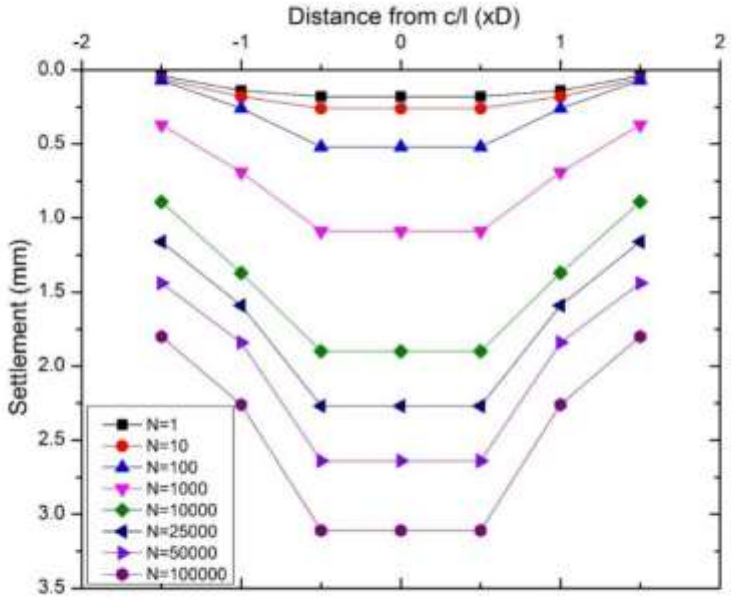

Figure 7.17 Surface deformation profile of reinforced test section (250mm)

The pressure acting on the subgrade with the applied pressure on the surface of the test sections is recorded with the help of the earth pressure cells installed similarly as in case of static loading test to understand the pressure distribution patterns. Figures. 7.18 and 7.19 presents the pressure distribution curves for unreinforced and reinforced case respectively. The pressure distribution curve gets sharper with an increase in number of loading cycles i.e. the pressure recorded exactly below the loading region is high. However, the pressure acting at a distance of 1D, 1.5D and 2D are relatively less.

It can observed that there is an increase in the pressure intensities recorded with an increase in number of loading cycles, it is because of the reason that initially there are chances of settlement in the base layer because of the load applied but as the loading cycles increased further there is less chance of settlement in base layer and more load is transferred to the subgrade. However, the pressure distribution patterns in the reinforced section are observed to be less narrow, unlike the pressure distribution patterns of unreinforced section. It can also be visualized that the pressure experiencing at the subgrade level at all the specified locations is less in reinforced pavement than the unreinforced. It indicates that the geocell reinforcement is capable of distributing the loads to a wider area which in turn helps in reducing the pressure intensities observed at the subgrade level. About a 20% reduction in the pressure was observed in the geocell reinforced test sections compared to the unreinforced test sections after 100000 loading cycles.

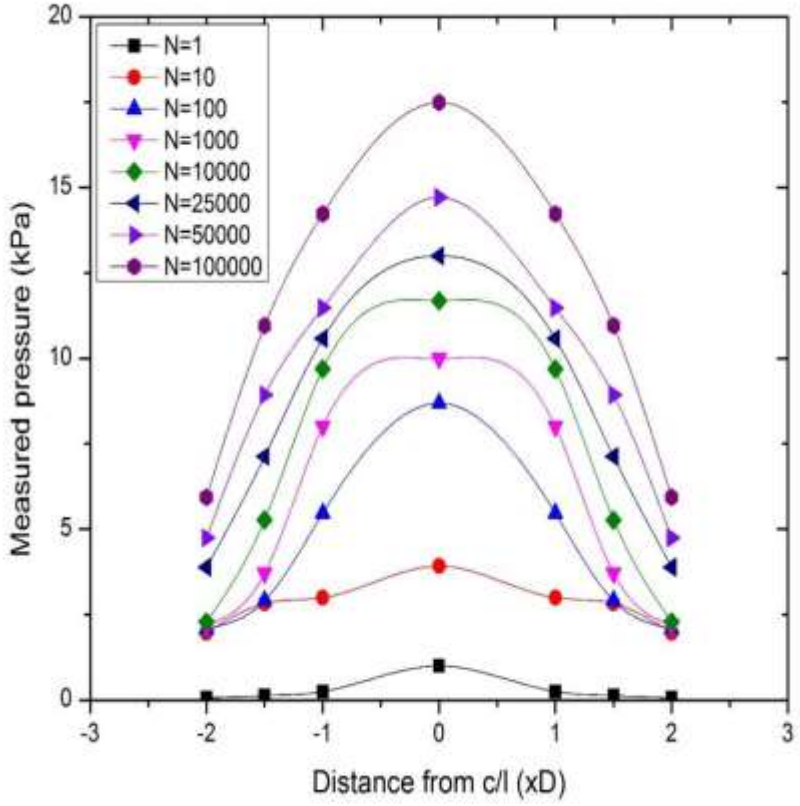

Figure 7.18 Variation of contact pressure measured at the base-subgrade interface for geocell reinforced test section (250mm)

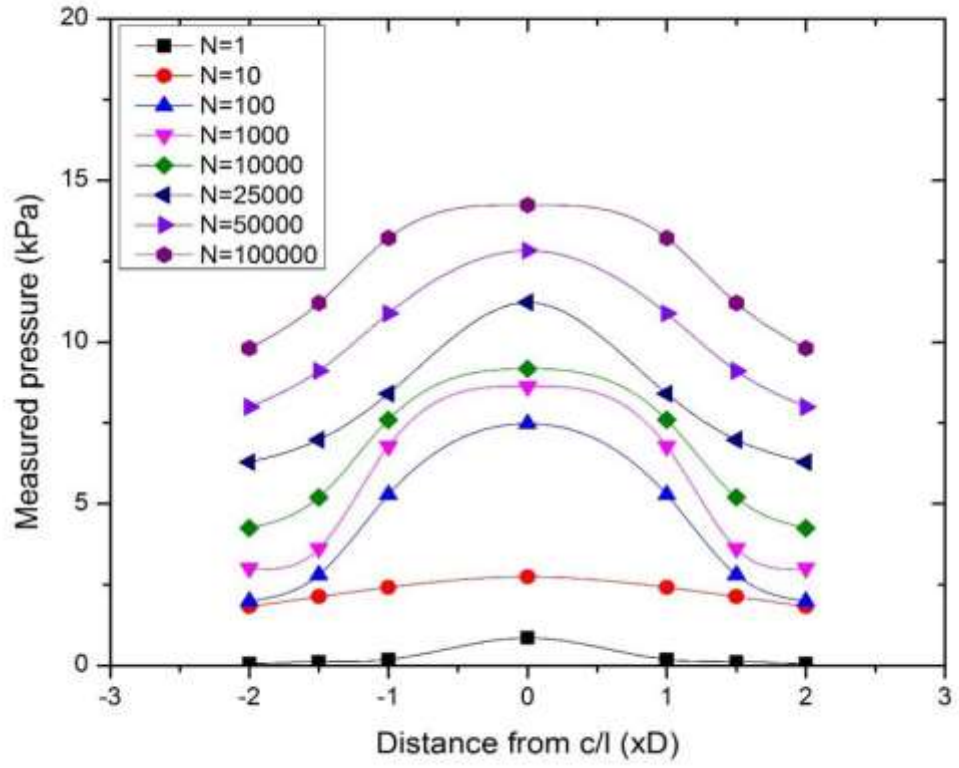

Figure 7.19 Variation of contact pressure measured at the base-subgrade interface for geocell reinforced test section (250 mm)

7.6 COST ANALYSIS

A detailed cost analysis has been carried out for the unreinforced geocell reinforced pavement sections. The cost of the granular base and bituminous layer are taken from the SOR for roads and bridge works of Tamil Nadu State Public Works Department. The cost analysis is carried out for two different test sections of a single lane flexible pavement and the results are tabulated in Tables 7.6 and 7.7 respectively. It can be seen that a net savings of Rs. 5,20,000 can be accounted for a km of reinforced flexible pavement section than the unreinforced pavement section. A reduction of about 17.01% were observed in the construction cost of a km stretch of flexible pavement.

Table 7.6 Cost analysis of a km stretch of unreinforced flexible pavement

Sl. No.	Description of items	Length (m)	Width (m)	Thickness (m)	Quantity of material (m^3)	Rate per unit	Price (Rs.)
1.	Wet Mix Macadam	1000	4.00	0.44	1760.00	4000/m^3	70,40,000.00
2.	Bituminous layer	1000	4.00	0.05	200.00	13000/m^3	26,00,000.00
	Total						96,40,000.00

Table 7.7 Cost analysis of a km stretch of geocell reinforced flexible pavement

Sl. No.	Description of items	Length (m)	Width (m)	Thickness (m)	Quantity of material	Rate per unit	Price (Rs)
1.	Wet Mix Macadam	1000	4.00	0.25	1000 m3	4000/m^3	40,00,000.00
2.	Bituminous layer	1000	4.00	0.05	200 m3	13000/m^3	26,00,000.00
3.	Geocell material	1000	4.00		4000 m^2	350/ m^2	14,00,000.00
4.	Total						80,00,000.00

7.7 SUMMARY

In this chapter, the results of the experiments conducted is discussed and is briefly explained the behaviour of the pavement sections with and without reinforcement. The performance in terms of TBR, RDR, RBR and also the cost analysis of both the pavement section is discussed.

VIII CONCLUSION

In the context of civil engineering construction, the prudent consideration of cost holds paramount importance. Upon a thorough examination of the cost analysis presented in the preceding chapter, it unequivocally reveals that reinforced pavement offers a 17.01% cost advantage over its unreinforced counterpart for every kilometre of single-lane road construction. The incorporation of Geocells within the base layer leads to a substantial 43% reduction in base thickness compared to unreinforced pavement, thereby diminishing the consumption of virgin materials, a resource of considerable scarcity.

Furthermore, Geocells prove instrumental in mitigating permanent deformations within the pavement structure by imparting added elasticity to the respective layers. This results in a noteworthy 13% reduction in cumulative permanent deformation within the reinforced pavement. Additionally, reductions of 13% in rut depth (RDR) and 19% in rut benefit ratio (RBR) underscore the Geocell's efficacy in distributing loads over a broader area, consequently minimizing rutting at the subgrade level.

Moreover, the observed equivalent modulus improvement factor stands at 1.3 times that of the unreinforced pavement section, indicative of the reinforced pavement's heightened stiffness, even while maintaining a reduced thickness profile. Attaining a Traffic Benefit Ratio (TBR) of 1.7 at a mere 50% permissible settlement (5 mm) after applying a 5% designed traffic load signifies the reinforced pavement's prolonged durability compared to its unreinforced counterpart under identical settlement conditions.

Finally, a layer coefficient ratio of 1.82 substantiates the comprehensive superiority of the Geocell-reinforced pavement section, featuring a reduced base thickness of 250 mm, over the unreinforced pavement section with a base thickness of 440 mm in all evaluated aspects.

It is worth noting that according to AASHTO standards, the thickness of the unreinforced pavement section is 553 mm as opposed to the 440 mm recommended by IRC for equivalent traffic repetitions. Given that Indian road designs predominantly adhere to IRC guidelines, there exists a potential for premature failures. This stems from the fact that IRC's calculations for resilient modulus in the base layer solely depend on the California Bearing Ratio (CBR) of the subgrade, overlooking the resilient modulus of the layer itself. In contrast, AASHTO methodology accounts for and designs based on actual resilient modulus values obtained from individual layers, a divergence from the IRC approach.

REFERENCES

[1] *https://en.wikipedia.org/wiki/Geo-synthetics*, accessed on 20/06/2017.

[2] *Webster, S. L. (1981).* Investigation of Beach Sand Trafficability Enhancement Using Sand-Grid Confinement and Membrane Reinforcement Concepts. Report 2. Sand Test Sections 3 and 4(No. WES/TR/GL-79-20). ARMY ENGINEER WATERWAYS EXPERIMENT STATION VICKSBURG MS GEOTECHNICAL LAB.

[3] *Carter, G. R. and Dixon, J. H. (1995).* Oriented polymer grid reinforcement. Construction and Building Materials, 9(6), 389-401

[4] *Biabani, M. M., Ngo, N. T., and Indraratna, B. (2016).* Performance evaluation of railway sub-ballast stabilised with geocell based on pull-out testing. Geo-textiles and Geomembranes, 44(4), 579-591.

[5] *Kim, Y. J., Jo, S. H., Lee, S. H., & Kim, N. (2013).* Field Applications on Environment-Friendly Permeable Pavements Reinforced by Geocell. Journal of Korean Society of Hazard Mitigation,13(2), 143-149.

[6] *Giroud, J. P., and Noiray, L. (1981).* Geo-textile-reinforced unpaved road design. Journal of Geotechnical and Geoenvironmental Engineering, 107. (ASCE 16489).

[7] *Barker, W. R. (1987).* Open-Graded Bases for Airfield Pavements (No. WES/MP/GL-87-16). ARMY ENGINEER WATERWAYS EXPERIMENT STATION VICKSBURG MS GEOTECHNICAL LAB.

[8] *Haas, R., Walls, J., & Carroll, R. G. (1988).*Geo-grid reinforcement of granular bases in flexible pavements (No. 1188). TRB, National Research Council, Washington, DC, USA, 19-27.

[9] *Al-Qadi, I. L., Brandon, T. L., Valentine, R. J., Lacina, B. A., & Smith, T. E. (1994).* Laboratory evaluation of geo-synthetic-reinforced pavement sections. Transportation Research Record, (1439).

[10] *Bush D.I., Jenner C.G. and Besset R.H.* The design and construction of geocell foundation mattress supporting over soft grounds, Geo-textiles and Geomembranes, Vol. 9, (1990) 83-98.

[11] *Barksdale, R. D., Brown, S. F., & Chan, F. (1989).*Potential benefits of geo-synthetics in flexible pavement systems (No. 315).

[12] *Cowland, J. W., & Wong, S. C. K. (1993).* Performance of a road embankment on soft clay supported on a geocell mattress foundation. Geo-textiles and Geomembranes, 12(8), 687-705.

[13] *Cancelli, A., &Cazzuffi, D. (1987).* Permittivity of geo-textiles in presence of water and pollutant fluids. In Proceedings of Geo-synthetics, Vol. 87, pp. 471-481.

[14] *Collin, J. G., Kinney, T. C., & Fu, X. (1996).* Full scale highway load test of flexible pavement systems with geo-grid reinforced base courses. Geo-synthetics International, 3(4), 537-549.

[15] *Dash, S. K., Krishnaswamy, N. R., and Rajagopal, K. (2001).* Bearing capacity of strip footings supported on geocell-reinforced sand. Geo-textiles and Geomembranes, 19(4), 235-256.

[16] *Sitharam, T. G., & Sireesh, S. (2005).* Behaviour of embedded footings supported on geo-grid cell reinforced foundation beds, 452-463.

[17] *Saride, S., Pradhan, S., Sitharam, T. G., &Puppala, A. J. (2013).* Numerical analysis of geocell reinforced ballast overlying soft clay subgrade. Geomechanics and Engineering, 5(3), 263-281.

[18] *Han J, Yang XM, Leshchinsky D, Parsons RL.* Behaviour of geocell-reinforced sand under a vertical load. Transportation Research Board J, (2008) No. 2045:95-101

[19] *Dash, S. K., Sireesh, S., &Sitharam, T. G. (2003).* Model studies on circular footing supported on geocell reinforced sand underlain by soft clay. Geo-textiles and Geomembranes, 21(4), 197-219.

[20] *Mandal, J. N., & Gupta, P. (1994).* Stability of geocell-reinforced soil. Construction and building materials, 8(1), 55-62.

[21] *Mhaiskar, S.Y., Mandal, J.N., 1994.* Three dimensional geocell structure: performance under repetitive loads. Proceedings of the 5th International Conference on Geo-textiles, Geomembranes, and Related Products, Singapore, pp. 155e158.

[22] *Rajagopal, K., Krishnaswamy, N.R., and Latha, G.M.* Behaviour of sand confined with single and multiple geocells. Geo-textiles and Geomembranes, (1999) 17(3), 171-184.

[23] *Hegde, A., & Sitharam, T. G. (2013).* Experimental and numerical studies on footings supported on geocell reinforced sand and clay beds. International Journal of Geotechnical Engineering,7(4), 346-354.

[24] *Halliday, A. R., & Potter, J. F. (1984).* The performance of a flexible pavement constructed on a strong fabric. TRRL LABORATORY REPORT, (1123).

[25] *Mengelt, M., Edil, T. B., & Benson, C. H. (2006).* Resilient modulus and plastic deformation of soil confined in a geocell. Geo-synthetics International,13(5), 195-205.

[26] *Pokharel, S. K., Han, J., Parsons, R. L., Qian, Y., Leshchinsky, D., & Halahmi, I. (2009, June).* Experimental study on bearing capacity of geocell-reinforced bases. In 8th international conference on Bearing Capacity of Roads, Railways and Airfields (pp. 1159-1166). June 2009: Champaign, IL, USA.

[27] *Tafreshi, S. M., & Dawson, A. R. (2010).* Comparison of bearing capacity of a strip footing on sand with geocell and with planar forms of geo-textile reinforcement. Geo-textiles and Geomembranes, 28(1), 72-84.

[28] *Pokharel, S. K., Han, J., Manandhar, C., Yang, X., Leshchinsky, D., Halahmi, I. & Parsons, R. L. (2011).* Accelerated pavement testing of geocell-reinforced unpaved roads over weak subgrade. Transportation Research Record, 2204, 67–75.

[29] *American Association of State Highway, & Transportation Officials. (1993).* AASHTO Guide for Design of Pavement Structures, 1993 (Vol. 1). AASHTO.

[30] *Korulla, M., Gharpure, A., &Rimoldi, P. (2015).* Design of geo-grids for road base stabilization. Indian Geotechnical Journal, 45(4), 458-471.

[31] *Technical Note:* "Development of Geo-grid Reinforced Flexible Pavement Layer Coefficient Ratios (LCRs) Based on Full Scale Trafficking Trials." Available at www.bostd.com.

[32] *IS 2720(PART4-1985)* Methods of test for soils: Sieve analysis of soil

[33] *IS-2720 (Part4-1972)* Methods of test for soils: Atterberg's limit of soil.

[34] *IS-2720 (Part3-1980)* Methods of test for soils: Specific gravity of soil.

[35] *IS-2720 (Part7-1980)* Methods of test for soils: Standard compaction test on soil.

[36] *IS 2720 (PART-16) 1987* Methods of test for soils: laboratory Determination of CBR

[37] *MORTH specification, 406.2.1.2.* (Table 400-11) 2000, Grading requirements of WMM.

[38] *IS-2720 (Part8-1980)* Methods of test for soils: Modified compaction test on soil.

[39] *Edil, T. B., Kim, W. H., Benson, C. H., &Tanyu, B. F. (2007).* Contribution of geo-synthetic reinforcement to granular layer stiffness. In Soil and Material Inputs for Mechanistic-Empirical Pavement Design (pp. 1-10).

[40] *Indian Road Congress, (2012).* Guidelines for the design of flexible pavements. Indian code of practice, IRC-37, New Delhi.

[41] *American Association of State Highway, & Transportation Officials. (2009).* AASHTO Standard Practice for Geo-synthetic Reinforcement of the Aggregate Base Course of Flexible Pavement Structures, AASHTO.

[42] *Krishnaswamy, N. R., Rajagopal, K., & Latha, G. M. (2000).* Model studies on geocell supported embankments constructed over a soft clay foundation.

[43] *Sireesh S.* Behaviour of Geocell Reinforced Foundation Beds Ph. D. Thesis, Indian Institute of science, Bangalore, 2005.

[44] *Tafreshi, S. M., & Dawson, A. R. (2012).* A comparison of static and cyclic loading responses of foundations on geocell-reinforced sand. Geotextiles and Geomembranes, 32, 55-68.

[45] *Yang, X., Han, J., Pokharel, S. K., Manandhar, C., Parsons, R. L., Leshchinsky, D., & Halahmi, I. (2012).* Accelerated pavement testing of unpaved roads with geocell-reinforced sand bases. Geotextiles and Geomembranes, 32, 95-103.